2005

An independent controller for active diesel exhaust aftertreatment.

Yue Wu
University of Windsor

AN INDEPENDENT CONTROLLER FOR ACTIVE DIESEL EXHAUST AFTERTREATMENT

by

Yue Wu

A Thesis
Submitted to the Faculty of Graduate Studies and Research
through Mechanical, Automotive and Materials Engineering
in Partial Fulfillment of the Requirements for
the Degree of Master of Applied Science at the
University of Windsor

Windsor, Ontario, Canada
2005

Your file Votre référence
ISBN: 0-494-09757-4
Our file Notre référence
ISBN: 0-494-09757-4

ABSTRACT

An independent controller was proposed to perform real-time diagnosis and modeling based control for diesel aftertreatment devices, such as the diesel particulate filters (DPF) and the lean NOx traps (LNT). The diesel aftertreatment devices for this research were in active flow control configuration. As opposed to passive aftertreatment control where the engine tailors the raw exhaust conditions, in active aftertreatment configuration, the raw exhaust conditions were modified with independent controls, such as aftertreatment temperature control, exhaust flow control, and aftertreatment excess air/fuel ratio (λ) control.

The determination of the diesel engine transient exhaust gas temperature is essential for effective active flow aftertreatment control schemes. To overcome the slow response of the high-inertia thermocouples used in the harsh diesel exhaust environment, a temperature response model was developed as part of this research. The temperature response model was verified by tests conducted on a Yanmar NFD170 single cylinder diesel engine setup. The model was then implemented into a National Instrument PCI-6023E multifunction data acquisition board with LabVIEW. The LabVIEW program was tested on the Yanmar engine setup and was capable of estimating the transient exhaust gas temperature in real-time using the temperature data obtained from two high-inertia thermocouples with a proper diameter ratio. The simplified transient aftertreatment model

representing the regeneration behavior of the DPF and the performance of the LNT were also proposed.

For this research, the aftertreatment device's substrate temperature, exhaust flow rates and direction, and the supplemental energy to the aftertreatment system were targeted to be controlled independently to enable energy efficient aftertreatment. To control the temperature of the aftertreatment device's substrate, a closed loop system was built to inject the proper amount of supplemental diesel fuel into the aftertreatment system. According to the property of its decision-making program, the substrate temperature control system could be operated manually or as an automatic system. Both the manual and the automatic substrate temperature control systems were tested successfully with the Yanmar diesel engine setup. The other components of the independent controller were also set up and tested individually. The experimental setup along with the preliminary empirical and theoretical results are reported.

DEDICATION

To my beloved husband,

Li Pan,

who provides unconditional love, everyday support and understanding.

ACKNOWLEDGEMENTS

The author wishes to express her heartfelt gratitude to Dr Ming Zheng and Dr Graham T. Reader for the supervision of this research, the guidance of this project, and for their support, guidance and understanding throughout the author's study in the master's degree program. Their valuable discussions and suggestions are deeply appreciated.

The author also wishes to express her appreciation to Ms. Jun Zuo, Mr. Raj Kumar, Mr. Dong Wang and Mr. Clarence M Mulenga for their time and helpful discussions. Many thanks are also due to Mr. Bruce Durfy, Mr. Suek Jin (Richard) Ko and Dr Guochang Zhao for their assistance with the instrumentation, and to Ms. Rosemarie Gignac and Mrs. Barbara Denomey for their continuous support at the departmental level.

This research is sponsored by the Canada Research Chair Programme, Canada Foundation of Innovation (CFI), Ontario Innovation Trust (OIT), Natural Sciences and Engineering Research Council of Canada (NSERC), AUTO 21^{TM} and University of Windsor.

TABLE OF CONTENTS

LIST OF TABLES

LIST OF FIGURES

NOMENCLATURE

A	Surface area, m^2
AC	Alternating current
ACV	Actuator throttle valve
C_p	Specific heat of the thermocouple junction, $kJ/(kg \cdot °C)$
CO	Carbon monoxide
CO_2	Carbon dioxide
d	Diameter of thermocouple wire, mm
DAQ	Data acquisition
DC	Direct current
DPF	Diesel particulate filter
e	Time averaged difference
ECU	Electronic control unit
EGR	Exhaust gas recirculation
Gr	Grashof number
G	Gradient of temperature readings
g/s	Gram per second
h	Convection heat transfer coefficient, $W/(m^2 \cdot °C)$
HC	Hydrocarbons
Hz	Hertz
i	Digitizing index of the temperature sampling time

IC	Integrated circuit
I/O	Input/Output
kS/s	Thousand samples per second
l/h	Liter per hour
LNT	Lean NO_x trap
m	Mass of the thermocouple junction, *kg*
$\dot{m}$	Gas mass flow rate, *g/s*
mA	Milliamp
MAF	Mass air flow
ml	Milliliter
ms	Millisecond
m/s	Meter per second
N	Number of samples
NI	National Instrument
N·m	Newton · meter
NPN	Negative-Positive-Negative
NO_x	Nitrogen oxides
$[NO_x]$	Nitrogen oxides concentration
Nu	Nusselt number
$[O_2]$	Oxygen concentration
ΔP	Pressure drop
PC	Personal computer

PM	Particulate matter
Pr	Prandtl number
PWM	Pulse Width Modulated
$\dot{Q}$	Heat transfer rate, W
Re	Reynolds number
rpm	Revolutions per minute
s	Second
t	Time, s
Δt	Time interval between two indexed temperature points, s
T	Thermocouple junction temperature, $°C$
ΔT	Temperature difference, $°C$
T_g	Gas temperature, $°C$
TTL	Transistor-transistor logical
TWC	Three-way catalyst
U	Fluid velocity, m/s
VI	Virtual instrument
WOT	Wide open throttle
λ	Excess air/fuel ratio
τ	Time constant of thermocouple, s
$\overline{\tau}$	Mean time constant of thermocouple, s
Σ	Abbreviate of $(1/N)\sum_{i=1}^{N}$

1. INTRODUCTION

Compared to gasoline engines, diesel engines are well known for their durability, robustness and low fuel consumption. The high thermal-efficiency of diesel engines results from their high compression ratios and overall fuel-lean operation. The high compression ratios generate a high temperature required to auto-ignite the diesel fuel and the resulting high expansion ratios lead to lesser thermal-energy discharged in the exhaust. As lean-burn engines, diesel engines have excess air/fuel ratios (λ) commonly between 1.2 and 1.5 on full loads and higher λ values as the loads reduce. When a modern diesel engine is idling, its λ can be an order of magnitude higher than that of stoichiometric engines *i.e.* $\lambda > 10$. The extra oxygen in diesel engine cylinders is necessary to enable complete combustion and to compensate for the non-homogeneity in fuel distribution. However, the diesel engine exhaust has a wide temperature range, normally from 100°C to 600°C, and high oxygen concentrations, between 5% and 20% [1].

In addition to the inherent high efficiency that leads to low emission level of carbon dioxide (CO_2), diesel engines emit low levels of carbon monoxide (CO) and hydrocarbon (HC) in the exhaust but emit relatively high levels of nitrogen oxides (NO_x) and particulate matter (PM) [2]. Although the diesel combustion is overall fuel-lean operation, in a microscopic sense, diffusion controlled diesel combustion is predominately a stoichiometric process because flame is tending to propagate towards approximately stoichiometric regions within an overall fuel-lean but heterogeneous mixture [2].

Therefore, the value of diesel engines flame temperature is close to that of the stoichiometric adiabatic flame temperature. In the presence of abundant oxygen and nitrogen, the high flame temperature produces large amount of undesired in-cylinder NO_x. Meanwhile, during the diffusion controlled diesel combustion phase, PM forms in the rich unburned-fuel-containing pockets of the non-homogeneous mixture approximating the flame region where the fuel vapor is heated by mixing with hot burned gases [2].

Although tremendous progress has been made in diesel engine technology in the past two decades, the reduction in engine-out NO_x and PM emissions can just barely keep up with the stricter emission standard. There are measures which can be taken to reduce the levels of NO_x or PM production, such as exhaust gas recirculation (EGR) for NO_x reduction and enhanced premixed combustion for PM decrease. However, some of the NO_x reduction approaches inevitably result in equally undesired increases in the levels of PM generation and may even deteriorate engine power performances. Conversely, some of the PM decrease methods unavoidably lead to raises of the levels of NO_x produced in-cylinder [1]. It seems that the improvement in diesel combustion alone may not be able to meet the next phase of emission legislation and therefore the aftertreatment devices are necessary.

Exhaust aftertreatment control strategies may be active or passive. In the modern automotive industry, the common practice is to use a passive aftertreatment system as shown in Figure 1-1 [3]. In the passive aftertreatment configuration, the engine has to cyclically generate an exhaust that is slightly lean or rich in oxygen to enable effective

operation of a three-way catalyst converter (TWC). This involves engine cyclic λ control, exhaust temperature skewing, and over-heat protection, in which the engine tailors raw exhaust conditions to satisfy aftertreatment schemes; therefore, the aftertreatment operation is monitored by the engine controller [3].

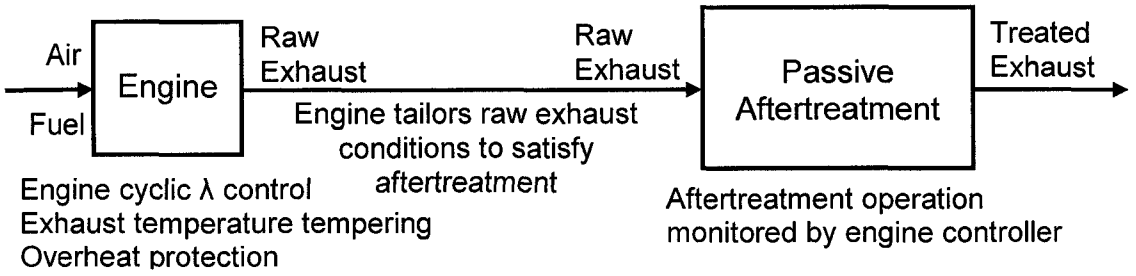

Figure 1-1 Passive aftertreatment system (after Zheng and Reader, 2004 [3])

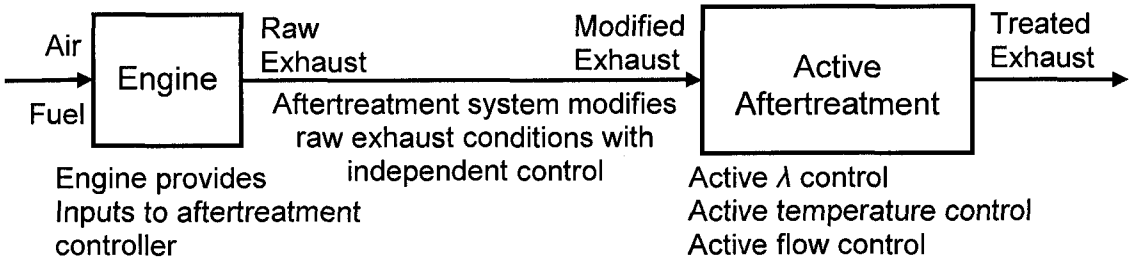

Figure 1-2 Active aftertreatment system (after Zheng and Reader, 2004 [3])

In an overall stoichiometric engine, the rich or lean pulses in the exhaust can be produced with little energy penalty. However, because the exhaust gas of diesel engines has a wide exhaust temperature range and is rich in oxygen, as mentioned previously, the generation

of rich pulses in the exhaust of diesel engines requires substantial amount of supplemental fuel which raises considerable energy penalties. To reduce the energy penalties, an active aftertreatment control strategy is proposed for diesel aftertreatment by Zheng and Reader [3]. In the active aftertreatment configuration, the aftertreatment system modifies the raw exhaust by an independent controller while the engine only provides the input for the aftertreatment controller, as shown in Figure 1-2 [3].

Active flow control aftertreatment, one of the active aftertreatment configurations, was proposed by Zheng and Reader [3]. Initial empirical studies conducted by Zheng and his coworkers [4-7] had indicated that the use of active flow control of the exhaust gases is a promising means to improve the performance of diesel aftertreatment devices. This concept was further investigated by developing an energy efficiency analysis that enabled investigation of the effects of different gas flow rates, flow reversal frequencies and monolith solid properties on aftertreatment performance. The simulation and empirical results indicated that through active thermal management the supplemental energy consumption could be drastically reduced by shifting the exhaust gas temperature, flow rate, and oxygen concentration to more favorable windows for the filtration, conversion, and regeneration processes of the aftertreatment devices.

Currently, at the author's laboratory, Clean Diesel Engine Technology Laboratory headed by Canadian Research Chair in Clean Diesel Engine Technology Dr Ming Zheng and Dean of Faculty of Engineering Dr Graham T. Reader, the active flow control

aftertreatment schemes that include parallel alternating flow, partial restricting flow, periodic flow reversal, and extended flow stagnation are under investigation. To realize the active flow control aftertreatment, an independent controller was proposed. Although the necessity of the independent controller was proved by the literature review [3-7], at the time of this report and after extensive search, no published literature with detailed technical schemes was found by the author concerning how to develop such an independent controller for the diesel aftertreatment.

The objective of this research is to develop an independent controller to conduct temperature control, exhaust flow control, and λ control for the diesel aftertreatment devices, which is shown in Figure 1-3. A temperature response model and simplified transient models of the aftertreatment devices are part of this research.

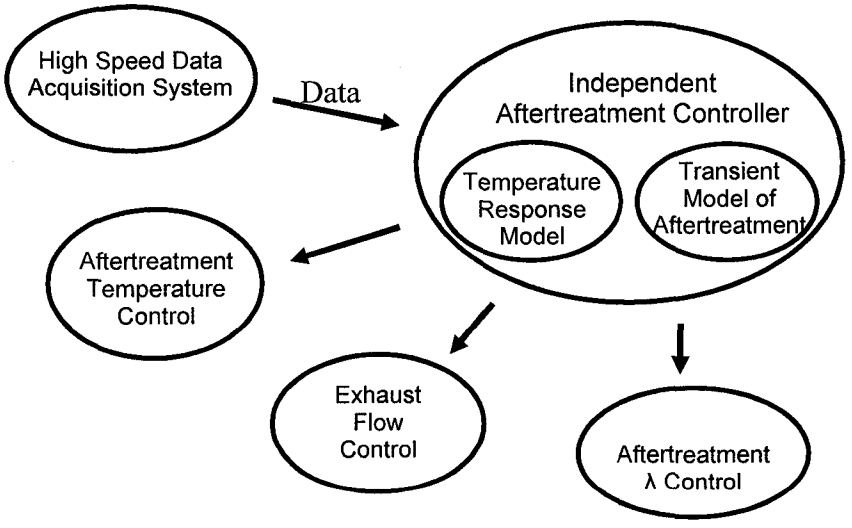

Figure 1-3 Research target

The overall control strategy of this research is reported in the next chapter, while Chapter 3 describes the experimental setup. Chapter 4 introduces the decision-making program, which consists of the two models of the independent controller, and presents the preliminary results of the models. In Chapter 5, after a simple closed loop system is introduced, the closed loop system for aftertreatment device's substrate temperature control is reported and the preliminary test results are documented. The last chapter includes the conclusions and recommendations.

2. OVERALL CONTROL STRATEGY

Although the objective of this research has been provided in Chapter 1, in order to fulfill the research target, it is necessary to define the detailed control strategy in this chapter. The exhaust gas of diesel engines has a wide exhaust temperature range and is rich in oxygen, which makes the conventional passive schemes incapable of energy-efficient aftertreatment. The active flow control aftertreatment system was proposed to reduce the supplement energy required to enable the diesel aftertreatment. The objective of this research is to develop an independent controller to conduct temperature control, and to prepare for exhaust flow control and λ control in the diesel aftertreatment devices such as the diesel particulate filter (DPF) and the lean NO_x trap (LNT).

To fulfill the objective of this research, a closed loop control system was proposed, as shown in Figure 2-1. A high speed data acquisition system was planned and partially implemented with a variety types of sensors placed in the aftertreatment and engine systems. Based on the feedback signals obtained from the data acquisition system, such as the temperature, the pressure and the exhaust NO_x and O_2 concentrations, the decision-making program of the independent controller will implement the control algorithm and generate four types of output signals. The four types of output signals included the amount of diesel fuel injected into the aftertreatment components, the on-set of an electrical heater, the directions and positions of exhaust flow valves, and the requirement

for the engine to supply more favorable conditions for the aftertreatment, such as to provide post injection [8].

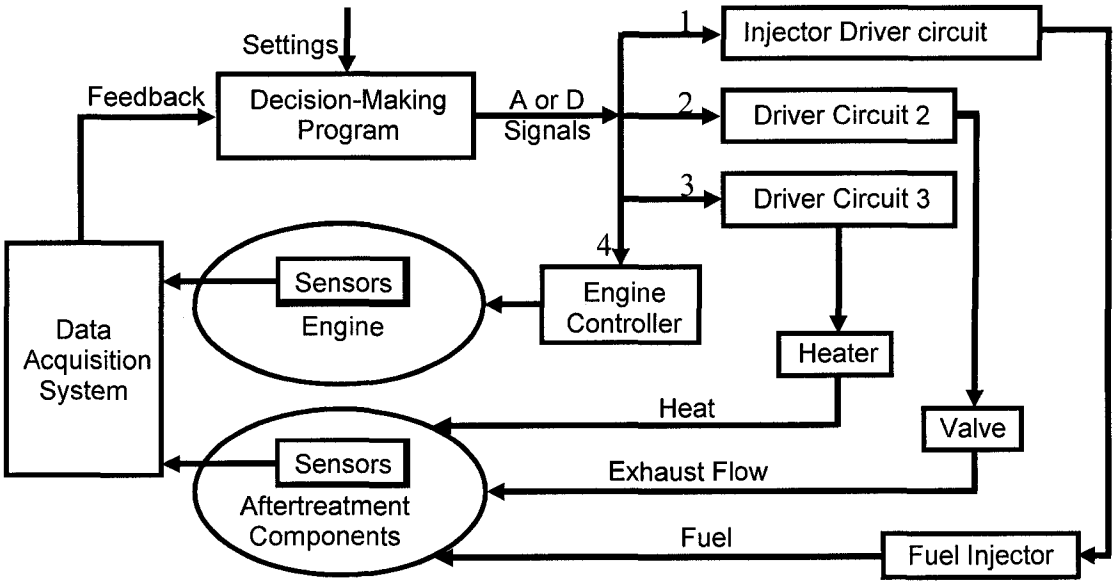

Figure 2-1 Closed loop system

The model-based independent controller intended to include two models, the first of which is the temperature response model and the second is the transient model of a DPF or a LNT. The temperature response model was to compensate the slow response of the durable temperature sensors, in this case with high inertia K-type thermocouples, in order to make the real-time control possible. The temperature response model was programmed into the decision-making program of the independent controller using LabVIEW and tested individually.

The second model in the independent controller was to represent the simplified transient behavior of a DPF or a LNT. Although the performance of the DPF and the LNT could be affected by many parameters, such as the substrate structure, material properties, engine exhaust gas temperature, exhaust gas flow rate, etc, only the most important parameters were included in the transient model. The engine exhaust temperature and the pressure drop across the DPF were considered in the DPF model, while the engine exhaust temperature, the exhaust gas mass flow rate, the exhaust NO_x concentration before the LNT and the exhaust O_2 concentration were considered in the LNT model. The basic concepts of the DPF and the LNT models were proposed, however, the DPF and the LNT models had not been implemented into the independent controller in this research, but been recommended as future work.

3. EXPERIMENTAL SETUP

The targeted aftertreatment control system will be tested on an engine dynamometer during this research project. The engine dynamometer setup provides the basis to implement the control strategy described in Chapter 2, although not the focus of this research. In this chapter, the experimental setup of the proposed independent controller for diesel aftertreatment is reported in detail. The sensors and the high speed data acquisition system are introduced first, followed by the descriptions of a fuel injector driver circuit. Then, a few different types of valves for exhaust flow control are presented. A fuel injector and its setup are reported at the end.

3.1. DATA ACQUISITION SYSTEM AND SENSORS

3.1.1. Sensors

A number of types of sensors have been planned to be placed into the aftertreatment system as well as the engine to collect the data needed. Table 3-1 summarizes data and sensors that were intended to be used in the aftertreatment controller, and the partial setup status of the sensors when this report is written.

3.1.1.1. Thermocouples

Type K thermocouples, with nickel-10% chromium as positive material and nickel-5% as negative material, had been chosen to be the temperature sensor for this research [9].

Type K thermocouple offers a wide temperature range, low standard error, and has good corrosion resistance while it is relatively inexpensive and easy to use. More than 30 type K thermocouples were placed into the exhaust pipe, the aftertreatment devices, and the engine. Most thermocouples were stainless steel sheathed while a few were bare-wired. Table 3-2 summarizes all the thermocouples used in this research. Mr. Clarence M Mulenga, a PhD candidate in the author's group, provided assistance in selecting and purchasing of the thermocouples.

Table 3-1 Data and sensors in the aftertreatment controller

No.	Data Name	Sensor	Status
1	Engine Exhaust Temperature	Thermocouples	Installed
2	Pressure (engine exhaust and after converter)	Pressure Transducer	Not installed
3	Aftertreatment λ	λ or O_2 sensor	Not installed
4	Exhaust flow rate	Mass air flow meter	Installed
5	Aftertreatment fueling rate	Fuel flow meter	Installed
6	Exhaust flow direction	Digital line	Installed
7	Exhaust composition	O_2 and NO_x sensors	Not installed
8	Engine speed	Encoder	Installed
9	Engine fueling rate	Fuel flow meter	Installed

Table 3-2 Summary of type K thermocouples

Type No.	Description
1	Omega CHAL-005 unsheathed fine gauge thermocouple, wire size 0.005"
2	Omega TJ36-CASS-116G-6 transition joint probe, grounded junction, junction and probe size 1/16"
3	Omega TJ36-CASS-18G-6 transition joint probe, grounded junction, junction and probe size 1/8"
4	Omega TJ36-CASS-140G-6 transition joint probe, grounded junction, junction and probe size 1/40"
5	ISSPRO R650 sheathed thermocouple, grounded junction, junction size 1/8", probe size 1/4"

3.1.1.2. Mass Air Flow Meter

A Bosch micromechanical HFM5 hot-film Mass Air Flow (MAF) meter, illustrated in Figure 3-1, was installed in the air intake system of the engine. The MAF meter is a thermal flow meter which produces voltage signals proportional to the mass air flow rates. The engine exhaust flow rate can be calculated based on the measured mass air flow rate and the engine fuelling rate. The MAF meter also has an integrated temperature sensor to determine the intake air temperature that will be used for future researches in the author's lab.

The power supply voltage of the MAF meter is +12V DC (direct current), and the reference voltage is +5V DC. The electronic interface of the meter has five pins which are temperature sensor output, power supply, power ground, reference voltage, and signal output, respectively [10]. M. A. Sc. candidate Mr. Suek Jin (Richard) Ko provided

assistance in obtaining the MAF meter, and PhD student Mr. Raj Kumar provided assistance in setting up the MAF meter.

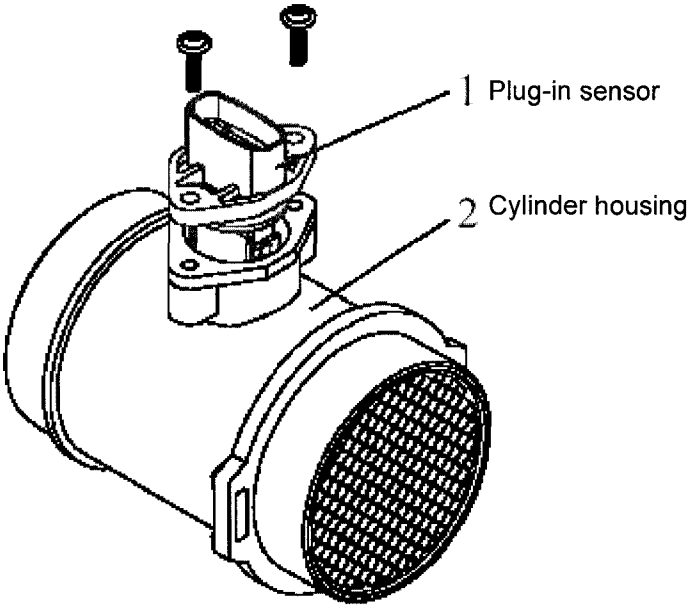

Figure 3-1 Bosch hot-film Mass Air Flow meter

3.1.1.3. Fuel Flow Meter

An ONO SOKKI fuel flow meter, which is a combination of a FP-2140H volumetric fuel flow detector installed at the fuel line and a DF-210A on-board digital flow meter, was set up to measure the fuelling rate of the engine and the aftertreatment devices. The meter is capable of measuring the instantaneous flow rate (positive displacement gear) and accumulated flow amount in high resolution, within ± 0.2% of the readings, with 0.3 to 120 liter per hour (l/h) measurement range [11].

The fuel flow meter, shown in Figure 3-2, is powered by a +12V DC power supply. In addition to its digital displays in the front panel for both instantaneous and accumulated flows, the meter can output two signals; 0 to 10V DC analog signals proportional to the instantaneous flow and a transistor-transistor logical (TTL) pulse train with every pulse representing 0.01 milliliter (ml) of the instantaneous flow [12]. Mr. Suek Jin (Richard) Ko provided assistance in selecting and purchasing the fuel flow meter, and Dr Guochang Zhao provided cooperation to set up the fuel line.

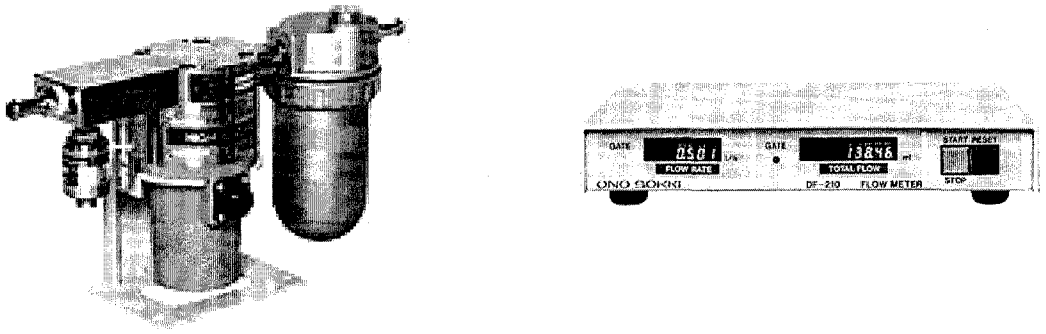

Meter and filter Display unit

Figure 3-2 ONO SOKKI fuel flow meter

3.1.1.4. Rotary Encoder

A Gurley 9125 optical rotary incremental encoder was mounted on the shaft of the engine to provide the engine angular speed. The encoder is designed for industrial-grade applications that require high resolution and high accuracy. For every crankshaft revolution, the encoder generates 3600 pulses and one zero index pulse. It uses +5V DC

power and has a 15-pin D-subminiature connector which provides the connections for two positive output pulse trains, two negative output pulse trains, one positive index pulse output, one negative index pulse output, the power input, and the common ground [13]. Mr. Raj Kumar provided assistance in the selection, purchase and installation of the encoder, and Mr. Clarence M Mulenga provided aid in the designing the coupler unit for the encoder.

3.1.2. Data Acquisition System

A high speed data acquisition system was set up, which consisted of a data acquisition unit and a signal conditioning unit. For the former part, a National Instruments (NI) PCI-6023E multifunction data acquisition (DAQ) board was inserted into the host personal computer (PC). In addition to eight digital Input/Output (I/O) lines and two 24-bit counters, the DAQ board provides 16 single-ended analog inputs with 12-bit resolution and a sampling rate up to 200 thousand samples per second (kS/s) [14]. The DAQ board can be programmed by NI LabVIEW, a fully functional graphical development environment with the flexibility of a traditional text-based language. A brief introduction of LabVIEW is provided in next chapter.

To protect the data acquisition board with isolation, and more importantly to improve data acquisition accuracy with amplification, filtering, and simultaneous sampling, an NI SCXI high performance signal conditioning system was installed between the sensors and the DAQ board. Figure 3-3 illustrates the data acquisition system layout and

Figure 3-4 is the picture of the signal conditioning system. The signal conditioning system includes an NI SCXI-1000 chassis, three NI SCXI-1102 thermocouple modules, three NI SCXI-1303 isothermal terminal blocks, an NI SCXI-1180 feed through panel and an NI SCXI-1302 terminal block. The chassis holds the three thermocouple modules and the feed through panel while the three isothermal terminal blocks and the 1302 terminal block are attached to the modules respectively.

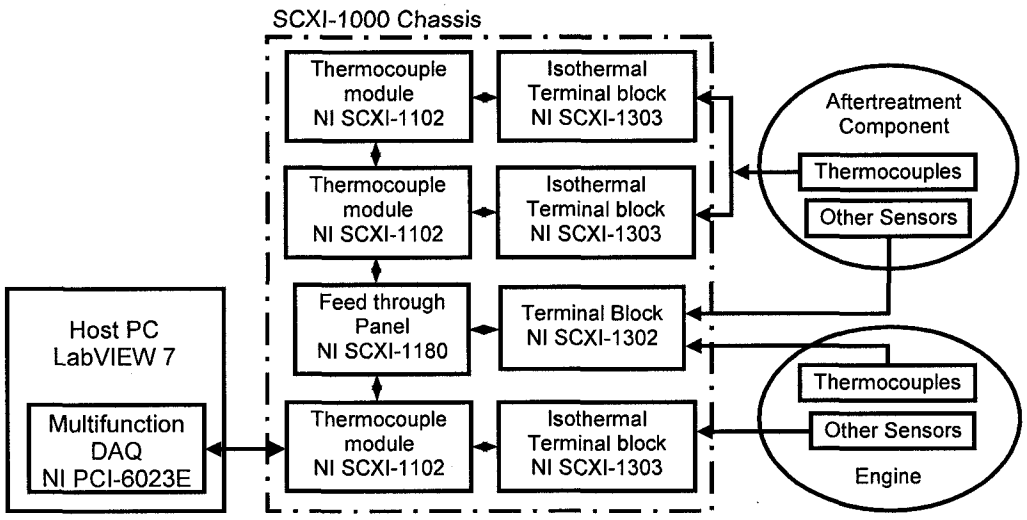

Figure 3-3 Data acquisition system layout

The NI SCXI-1102 thermocouple module is designed for high-accuracy temperature measurement for thermocouples only (type-J, K, N, R, S, T, B, E). Each module has 32 input channels each of which includes an instrumentation amplifier and a 2 Hz low pass filter. SCXI-1102 module can also acquire millivolt, volt, and 4 to 20 milliamp (mA) current input signals with scan rate up to 333 kS/s. Each module multiplexes its channels

into a single channel of the DAQ board, and makes it possible to add more modules to increase channel count [15].

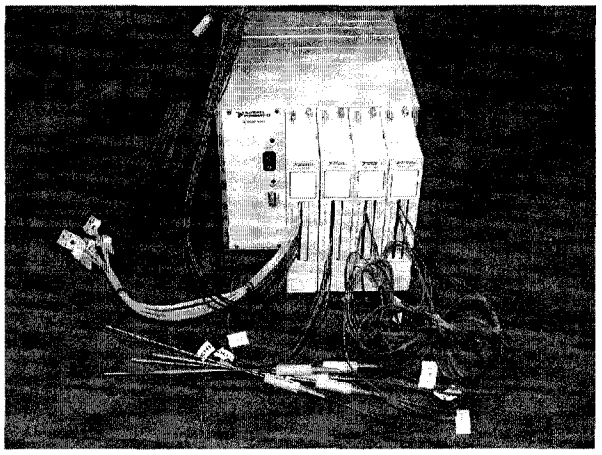

Figure 3-4 NI SCXI signal conditioning system

The NI PCI-6023E DAQ board and all the NI SCXI modules was accessed with the NI Measurement & Automation Explorer (MAX) software. MAX was used to configure the NI hardware and software; create and edit channels, tasks, interfaces, scales and virtual instruments; view devices and instruments connected to the system, and execute system diagnostics.

3.2. FUEL INJECTOR DRIVER CIRCUIT

A fuel injector driver circuit was built to control the opening and closing of the fuel injector with the transistor-transistor logic (TTL) pulses as the input signal. The schematic diagram of the circuit is shown in Figure 3-5. Figure 3-6 is the picture of the circuit board. The major component of this circuit is the LM1949 linear integrated circuit (IC) from National Semiconductor Corporation. The IC controls an external power Negative-Positive-Negative (NPN) Darlington transistor that drives the high current injector solenoid. This driver circuit is capable of amplifying the input TTL signal in a high degree of correlation and maintaining the sharp rise and drop edges in the output signal. Therefore, the opening and closing delay of the fuel injector is reduced.

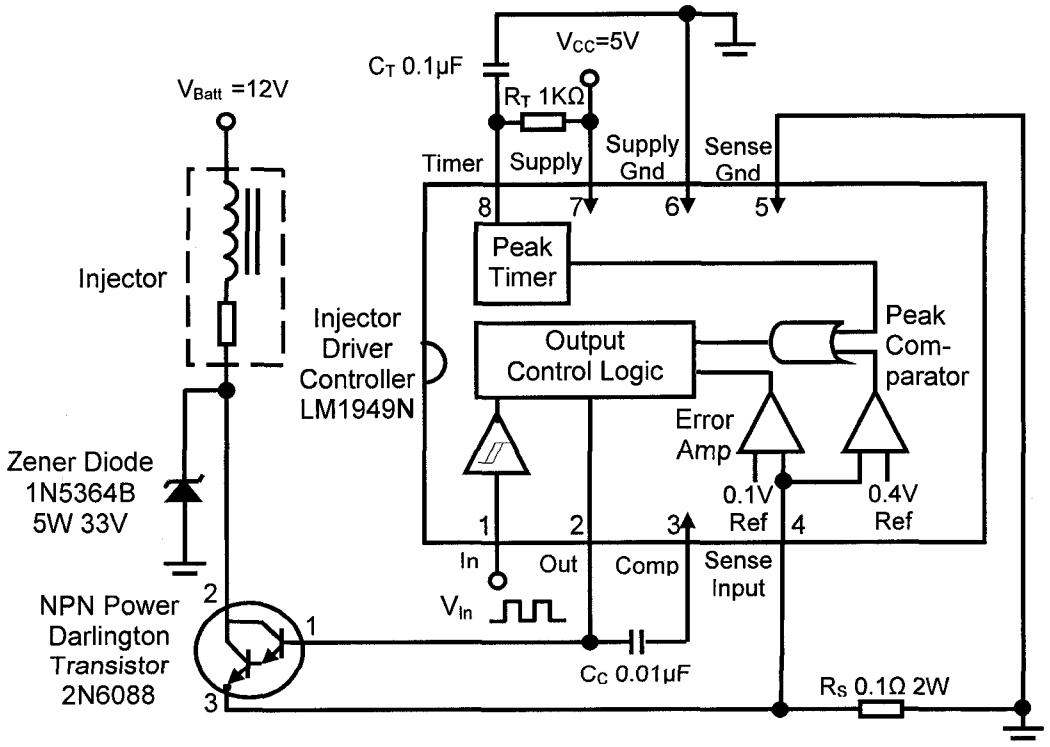

Figure 3-5 Schematic diagram of the injector driver circuit

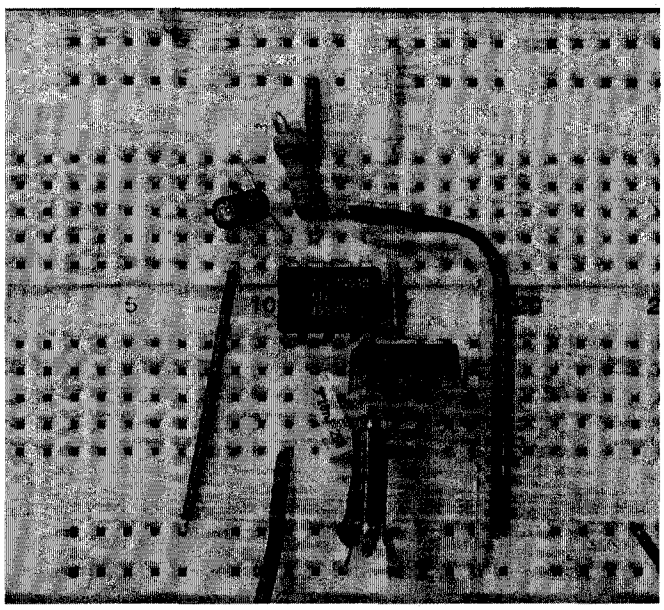

Figure 3-6 Injector driver circuit

A fuel injector can usually be modeled by an inductor and a resistor connected in series as shown in Figure 3-5. In actual operation, the inductance of the injector will change depending upon the status of the solenoid. Usually, the current required to open a solenoid is several times greater than the current necessary to merely hold it open.

The input signal of this circuit is the fuel injector control signal from the independent controller and is applied to Pin 1 of the IC. The input signal is in the form of a TTL square wave with a variable duty cycle (duty cycle = high time of the pulse / period of the pulse) and/or variable frequency, which is proportional to the amount of diesel fuel needed in the aftertreatment devices.

When the IC senses a logic 1 signal at Pin 1, it drives the Darlington transistor into saturation. The injector current will rise exponentially from zero and the voltage drop across the sense resistor R_S will raise with the current. When this voltage reaches 0.4 V, the IC changes from the peak state into the hold state. In the latter state, the IC behaves as an operational amplifier and drives the Darlington transistor within a closed loop system to maintain the hold reference voltage, typically 0.1 V, across R_S [16].

Once the injector current decreases from the peak level to the hold level, it remains there for the duration of logic 1 of the input signal at Pin 1. This type of operation is preferable since the current required to overcome the kinetic and constriction forces is often a factor of multiple times of the current needed to hold the injector open. By holding the injector current at one fourth of the peak current, power dissipation in the solenoids and the Darlington transistor is reduced by at least the same factor.

3.3. EXHAUST FLOW CONTROL VALVES

To control the exhaust flow of the aftertreatment, two types of valve actuation mechanisms were prepared: the smart actuator throttle valves from Siemens and the solenoid valves from Parker.

3.3.1. Smart Actuator Throttle Valve

The smart actuator throttle valves (Smart ACV) from Siemens can be used to accurately control the exhaust flow rates of the aftertreatment devices by adjusting the position of

the throttle valve. The ACV valve, shown in Figure 3-7, was referred as "smart" because an external power driver circuit for the input signal and an external position sensor for closed loop control are not required. The Smart ACV was originally developed to serve as a smart component in an Engine Control Unit (ECU) for modern industry combustion engines. The actuator enclosure holds a high-temperature tolerate ECU internally, which controls the throttle valve position according to the input signal, registers the actual valve position value, runs an error detection program, and controls the on-board DC motor [17].

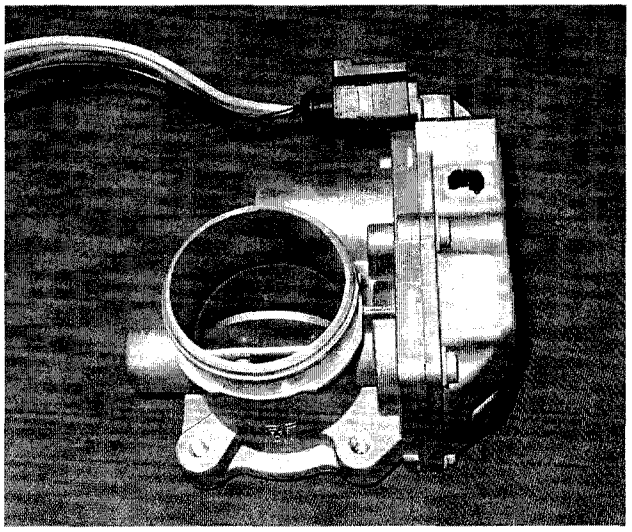

Figure 3-7 Smart actuator throttle valve

The throttle valve is driven by the integrated DC motor with a two-step gear. The digital position control inside the Smart ACV is designed as a software on the ECU. It drives the DC motor directly through the final output stages. The actual throttle valve position is registered by a non-contact sensor, and a reset spring places the de-energized throttle valve in its fully open position. If the integrated ECU detects an error, the throttle valve

will be moved to the wide open throttle (WOT) position and a status return signal will be sent out [17].

The operating voltage of the Smart ACV is from 9V to 17V DC, and the electronic interface of the Smart ACV is a four-pin connector. These four pins include the power supply, the power ground, the status return signal and the input Pulse Width Modulated (PWM) signal. The input signal is considered high level when its voltage is higher than 80% of the supply voltage, which is higher than 7.2V. When its voltage is lower than 2V, the input signal is treated as low level. The frequency of the input PWM signal has to be rated at 250Hz ± 3%. If the PWM frequency is outside the specifications, the throttle valve will be moved to its WOT position, and the status return signal will be sent out. The opening position of the throttle valve is defined by the duty cycle of the PWM signal as summarized in Table 3-3 [17].

Table 3-3 Summary of the PWM duty cycle and the throttle valve position

PWM Duty Cycle	Throttle Valve Position
5% ~ 94 %	Normal operations (5%: throttle valve fully open; 94%: throttle valve closed)
94% ~ 95%	Maintaining the last valid throttle valve position
95% ~ 97%	Throttle valve fully closed
Remaining duty cycles	Throttle valve fully open and error signal output on the status line, if duty cycle < 3% or > 97%.

The Smart ACVs were tested successfully by feeding proper PWM signals to them. The PWM signals were generated by the NI PCI-6023E DAQ board programmed with NI LabVIEW.

3.3.2. Solenoid Valve

Another type of exhaust control valve prepared for the independent controller is the Gold Ring series 30 universal three-way direct acting solenoid valve manufactured by Parker Hannifin Corporation, shown in Figure 3-8. The solenoid valve is powered by 12 to 24 V DC and pressure can be placed at any port [18]. Figure 3-9 is the flow diagram of the solenoid valve, which shows that ports 1 and 3 are connected when it is de-energized and ports 1 and 2 are connected when energized.

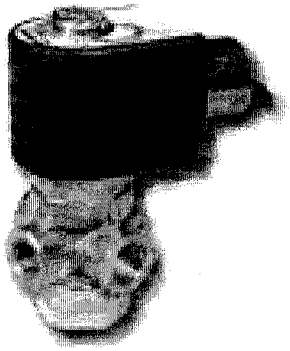

Figure 3-8 Three-way direct acting solenoid valve

Two solenoid valves were set up to control the directions of the exhaust flow of the aftertreatment devices as summarized in Table 3-4. The NI LabVIEW was programmed to generate two digital signals by the NI PCI-6023E DAQ board. Each digital signal was then amplified by one fuel injector driver circuit to control the movement of one solenoid

valve. Mr. Dong Wang, a PhD student in the author's group, provided assistance in the purchase and setup of the solenoid valves.

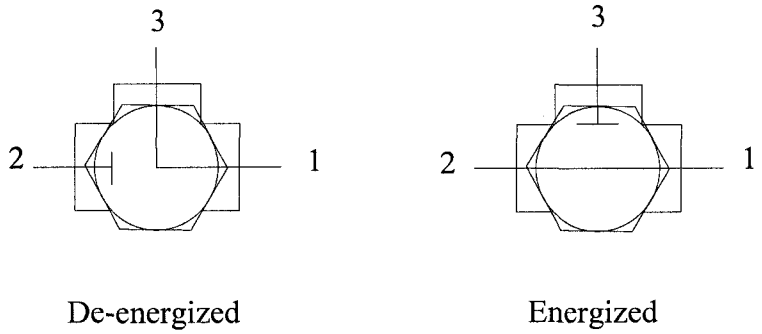

De-energized Energized

Figure 3-9 Flow diagram of the solenoid valve

Table 3-4 Summary of the set up of the solenoid valves

No.	Valve 1	Valve 2	Exhaust Flow Conditions
1	On	Off	Forward flow
2	Off	On	Backward flow
3	Off	Off	Bypass flow

3.4. FUEL INJECTOR

To inject diesel fuel into the aftertreatment devices, a Delphi gasoline fuel injector from a Ford passenger car was calibrated and set up.

3.4.1. Fuel Injector Calibration

To calibrate the fuel injector, city tap water which was pressurized by the compressed air available in the lab was supplied to the injector. The pressure of the water was adjusted by changing the pressure of the compressed air through an air pressure regulator. Generated by the NI PCI-6023E DAQ board programmed with NI LabVIEW, TTL pulse trains with desired frequency and duty cycle were amplified by the fuel injector driver circuit and fed to the fuel injector to control its opening and closing.

For each test condition based on the water pressure, injector input voltage, pulse frequency, duty cycle and pulse number, the water injected by the fuel injector was collected, weighed and recorded. The mass flow rate of water, thus obtained at each test condition was converted into the volume flow rate and finally the equivalent mass flow rate of diesel fuel was determined. Multiple injection shots were collected to improve the measurement accuracy. Figure 3-10 shows the fuel injector calibration results with 12V DC input voltage.

3.4.2. Fuel Injector Setup

The fuel injector was originally designed to work in the engine intake environment and therefore could not tolerant the high temperature present in the diesel engine exhaust system. To achieve the direct injection of the diesel fuel into the exhaust pipe and to protect the fuel injector from the high exhaust temperature, a water cooled stainless steel

fuel injector adapter was built. Figure 3-11 illustrates the structure of the fuel injector adapter and Figure 3-12 is the picture of the fuel injector setup.

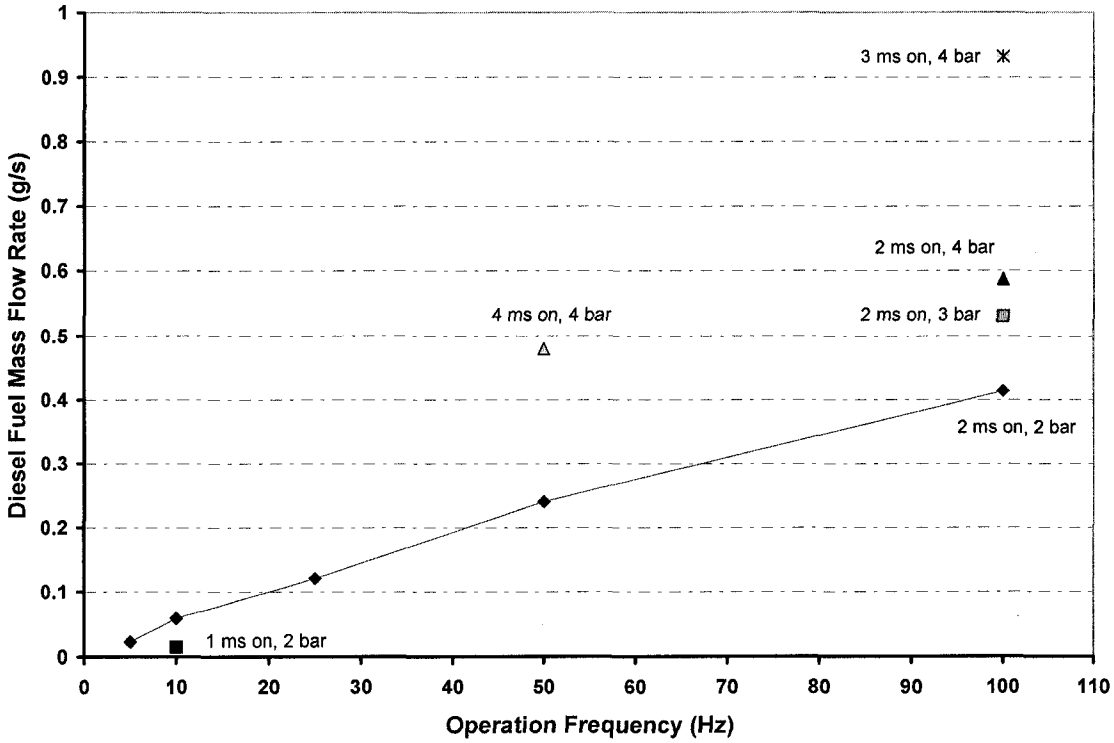

Figure 3-10 Fuel injector calibration results

City tap water was used as the coolant to take away the extra heat from the injector, while a 1/16" diameter thermocouple was installed to monitor the temperature of the coolant constantly to prevent overheating. During the experiments, the temperature of the fuel injector was successfully maintained below 110°C, the upper safe temperature limit. Figure 3-13 shows the temperatures of engine exhaust gas and the fuel injector coolant during one of the engine tests.

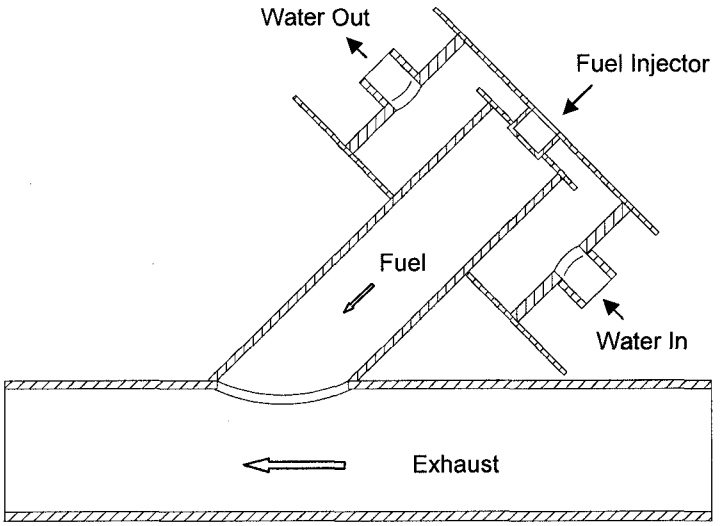

Figure 3-11 Schematic diagram of the fuel injector adapter

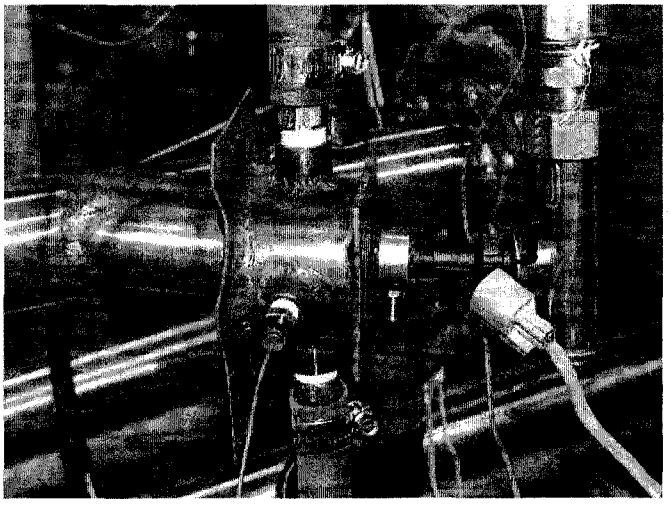

Figure 3-12 Fuel injector adapter

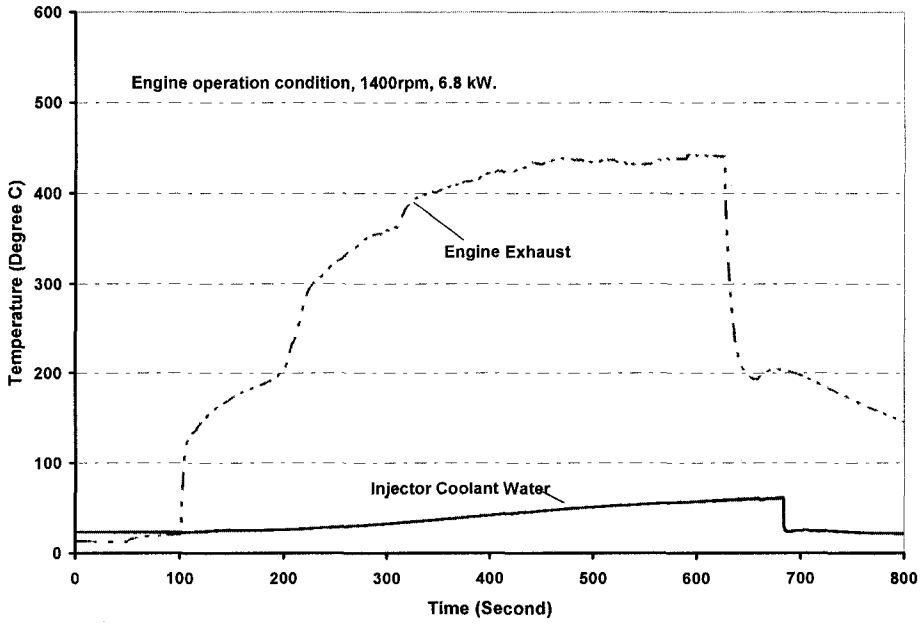

Figure 3-13 Engine exhaust temperature and fuel injector coolant water temperature during one engine test

4. DECISION-MAKING PROGRAM

The decision-making program contains the software configuration and control algorithm of the proposed independent aftertreatment controller. It defines how the independent controller functions and consists of the data acquisition, control algorithm and signal output functions. In this chapter, the first section is a brief introduction of the National Instrument (NI) LabVIEW in which the decision-making program was written. The development and implement of a temperature response model which is a major part of the algorithm is reported in detail. After that, the basic concepts of a simplified transient diesel particulate filter (DPF) model and a lean NO_x trap model are reported. The last section describes the decision-making program layout and the functionality of each of the three parts of the program.

4.1. NATIONAL INSTRUMENT LABVIEW

NI LabVIEW is a graphical development environment for designing test, measurement, and control systems, giving its users the flexibility of a programming language without the complexity of traditional development tools. NI LabVIEW has been popular in the industries worldwide, including automotive, telecommunications, aerospace, semiconductor, electronic design and production, process control, and biomedical application [19].

Designed specifically for the creation of flexible and scalable test, measurement and control applications, rapidly and at a minimal cost, LabVIEW is a fully functional graphical programming language. As the basic building block of a LabVIEW application, a virtual instrument (VI) consists of a front panel and a block diagram. In the front panel users can design their own user interface, and in the block diagram, they can create the graphical code. Figure 4-1 shows the front panel of a VI, while Figure 4-2 illustrates the block diagram of the same VI. Since LabVIEW VIs are modular in design, each of them can be run by itself or as a subVI. Therefore, LabVIEW applications can conveniently be scaled from simple applications to highly sophisticated systems [19].

The execution order of a LabVIEW program is determined by the flow of data between nodes instead of the sequential lines of text because of the patented dataflow programming model of LabVIEW. Since LabVIEW has a compiler that generates optimized code with execution speed comparable to compiled C programs, the execution speed of LabVIEW program is not sacrificed for the convenient graphical programming environment. Most importantly, LabVIEW is supported by a full line of NI hardware, including real-time, PXI, data acquisition, signal conditioning, motion and vision modules and systems, and many third parties hardware. Therefore, a LabVIEW application can be easily transferred from the desktop to a handheld device, and from a real-time to an embedded device as a stand-alone executable [19].

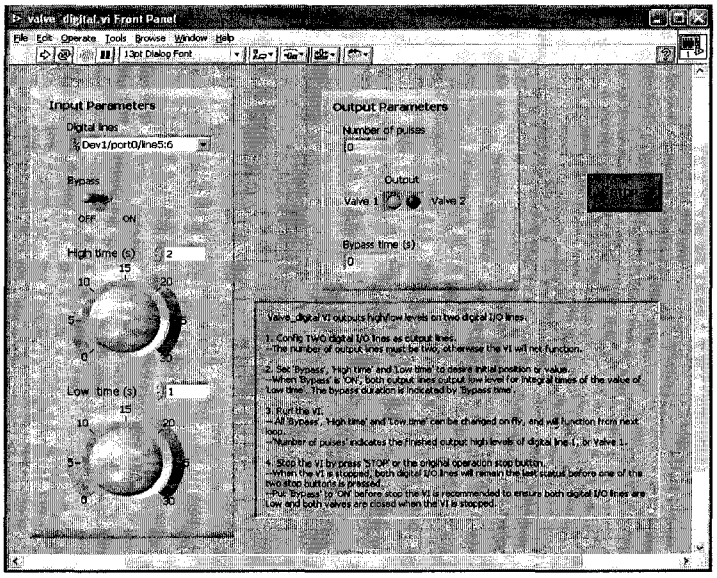

Figure 4-1 Front panel of a virtual instrument (VI)

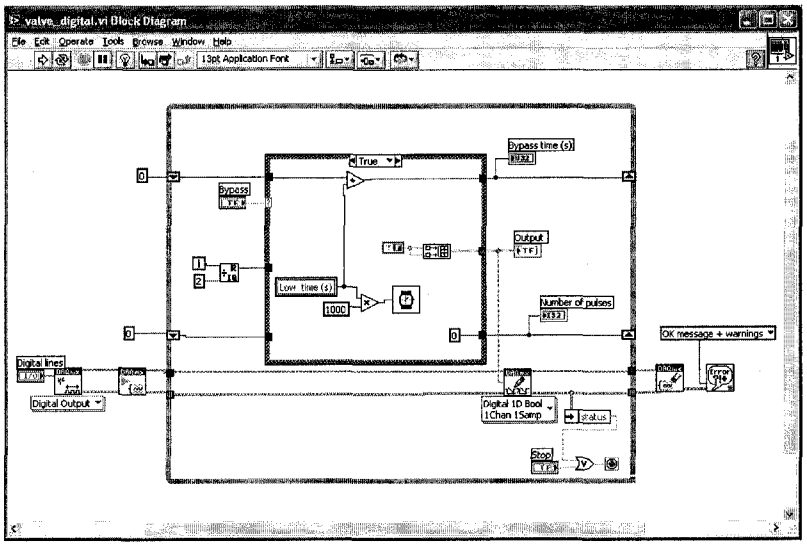

Figure 4-2 Block diagram of a virtual instrument (VI)

4.2. TEMPERATURE RESPONSE MODEL

Diesel engine exhaust temperatures vary with the engine load and speed, which affects the thermal behavior and thus the performance of the exhaust aftertreatment systems. The determination of exhaust gas transient temperature is, therefore, essential for effective active-flow aftertreatment control schemes. In addition, exhaust gas temperature measurements for detecting catalyst light-off performance could allow for enhanced monitoring and reduction of emissions during some vital phases. The measured exhaust temperature could also be used as an input for the various engine management functions, such as the catalyst temperature control, the catalyst over-temperature protection, the air/fuel ratio control, the diesel particulate filter (DPF) regeneration control and the over-temperature protection for lean NOx trap (LNT). Therefore, as the requirement for the diesel engine exhaust emissions becomes increasingly stringent, the accurate measurement of exhaust gas temperature becomes critical for the diesel engine management and the aftertreatment control systems.

Critical challenges existed with real-time engine exhaust gas temperature measurements when using thermocouples or other kind of temperature sensors. The major difficulty is the conflict of the fast response to the transient temperature and the durability of the thermocouple in high temperature and reactive gas flow fields. To realize a fast-response to the dynamic temperature variations, lower inertia thermocouples are desired. However, this requires thinner thermocouple wire junctions that commonly can not meet the extended durability requirements in reactive gas environment. Furthermore, diesel

exhaust gases impose a harsh environment that in combination with the low cost and robust requirements excludes many of the fast response temperature sensors from automotive use. To meet the extensive durability requirement of the diesel aftertreatment conditions, a common practice in the modern diesel automotive industry is to use thick thermocouples in the exhaust system, such as the 1/4" diameter thermocouples. Nevertheless, the response of the thick thermocouples to the temperature fluctuation is far too slow to fulfill the requirement of the aftertreatment and engine management. Mathematic prediction of the transient temperature using a temperature response model is one of the popular choices to enable the estimation of the real-time exhaust temperature with high inertia thermocouples.

4.2.1. Temperature Response Model Development

4.2.1.1. Thermocouple Time Constant

For a specifically designed thermocouple probe, inserted sufficiently long into the exhaust flow field, with appropriate thermal insulation between the exhaust pipe and the thermocouple tube as well as between the thermocouple tube and the ambient air (outside the exhaust pipe), the effect of heat transfer by conduction could be neglected compared to the prevailing effect of heat transfer by convection across the thermocouple bead. Noting that diesel engine exhaust temperature is commonly in the range of 100 °C~600 °C, the effects of radiation heat transfer between the thermocouple, the exhaust pipe, and the exhaust stream could also be neglected because of the relatively low temperature and

limited temperature differences. Thus, considering heat transfer by convection only, the rate of heat addition equals the rate at which heat is being stored in the thermocouple junction [20]:

$$hA(T_g - T) = mC_p \frac{dT}{dt} \tag{1}$$

where h is the convection heat transfer coefficient in $W/(m^2 \cdot °C)$, A is the surface area through which convection heat transfer takes place, T_g is the gas temperature, T is the thermocouple junction temperature, m is the mass of the thermocouple junction, and C_p is the specific heat of the junction.

Defining a time constant τ as

$$\tau = \frac{mC_p}{hA} \tag{2}$$

and rearranging Equation (1), we can get:

$$T_g = T + \tau \frac{dT}{dt} \tag{3}$$

By using this relationship, thermocouple readings (T) can be corrected to yield the exhaust gas temperature (T_g) if τ is known.

The convection heat transfer coefficient h plays an essential role in estimating the time constant and is usually given by a non-dimensional expression for its Nusselt number, *Nu*. The Nusselt number can be represented as a function of the Reynolds number *Re*, the Grashof number *Gr*, the Prandtl number *Pr*, etc.: *Nu= Nu (Re, Gr, Pr . . .)* [21]. Then, the

time constant, τ, is a function of the fluid velocity U, the fluid temperature T_g, the thermocouple wire diameter d, and other parameters.

$$\tau = f(U, T_g, d, ...) \quad (4)$$

4.2.1.2. Estimation of Transient Temperature

The major difficulty in estimating the fluctuating gas temperatures by using high inertia thermocouples is to determine the time constants of the thermocouples in an active velocity and thermal field. Noticeably, the time constant is actually a variable under the exhaust gas flow conditions. Extensive research has been carried out for overcoming this difficulty. The techniques for estimation of transient temperatures can be broadly divided into two categories: estimation of transient temperature by using a single thermocouple and estimation of transient temperature by using two thermocouples [20, 22-39].

4.2.1.2.1. Estimation of Transient Temperature by Using a Single Thermocouple

When a single thermocouple is used to estimate the transient temperature, the most common practice is to use a mean time constant of the thermocouple for a certain flow range in which the research is carried out [20, 22-25]. Special procedures are required to determine the mean time constant in advance, such as internal heating procedures and external heating procedures.

Internal heating procedures involve two steps: heating the thermocouple junction and wires by applying an AC (alternating current) or DC current, and observing of the decay in junction temperature after removal of the heating current [22, 23, and 25]. These procedures probably are the most widely used methods to determine the thermocouple time constant even the procedures clearly do not allow time constant determination while the thermocouple is heating. In addition, the procedures suffer from uneven internal heating of the junction and wires. A delay is needed to allow the temperature of the junction and wires to become more homogeneous. By only measuring the time constant after a delay of half or one time constant period after removing the heating current, some of the disadvantages may be overcome [26]. However, the use of such a delay limits the maximum junction and wire temperature at which the time constant can be measured to approximately half of the initial temperature at the time of removal of the heating current.

In the external heating procedures, the time constants of thermocouples are determined by examining the thermocouple responses to known changes in the surrounding fluid temperatures [20 and 24]. These procedures obviously allow determination of the thermocouple time constants during both heating and cooling; however, they require accurate knowledge of the external temperature field.

Since the mean time constant is determined by undergoing specific procedures with a specific thermocouple, the physic properties of the thermocouple junction, such as junction size and material densities, are critical to the application. For instance, after a

long period of operation, a thermocouple probe inserted into the exhaust pipe near the exhaust valve of a diesel engine would be covered by a thick layer of soot, which will affect the response of the thermocouple to the fluctuating temperature. At this stage, more errors will be introduced in the estimation of the transient temperature in addition to the errors brought in with the use of the mean, instead of real-time, time constant of the thermocouple.

4.2.1.2.2. Estimation of Transient Temperature by Using Two Thermocouples

From 1976, different methods have been developed to deduce the thermocouple time constant by comparison of the response of two thermocouples with unequal time constants subjected to identical external temperature fluctuations [27-31]. Either the mean time constant or the real-time time constant is used to estimate the transient temperature with two thermocouples. Besides the necessity of installing an additional thermocouple at close proximity, no requirement for the accurate knowledge of the external fluid temperature field and almost no specific procedures are needed to determine the time constant.

Strahle and Muthukrishnan [27] have shown that the mean thermocouple time constants may be found by examining the ratio of the auto-spectral density function of the signal from one thermocouple to the cross-spectral density function of the first signal and a second signal from the second thermocouple with a distinct time constant located in close proximity. Cambray [28] introduced another scheme to estimate the instantaneous time

constant which relies on the assumption that the ratio of time constants of two thermocouples remains approximately constant with temperature. Forney and Fralick [29] tested a scheme similar to Cambray's. Nevertheless, these techniques have serious difficulties when applied to the actual temperature measurement of a turbulent combustion process. In 1997, Tagawa and Ohta [30] presented a new method to estimate the thermocouple time constants and to compensate the thermocouple response simultaneously using two fine wire thermocouples in a combustion wind tunnel. Santoni, Marcelli and Leoni [31] expanded Tagawa and Ohta's method by taking radiation into account and applied the method to continuous flame spreading across a fuel bed. Similar approaches could be developed to other transient temperature measurement scenarios such as the engine exhaust gas. Thus, the development of a mathematical model to estimate the diesel engine transient exhaust gas temperature is given below.

4.2.1.3. Temperature Response Model Development

In this investigation, two thermocouples of different diameters are placed with their junctions a few millimeter from each other and mounted in a radial configuration in the exhaust pipe, as illustrated in Figure 4-3. The following set of equations for estimating the exhaust gas temperatures T_{g1} and T_{g2} could be applied. Similar approaches were reported previously by other researchers [30]:

$$\left.\begin{aligned} T_{g1} &= T_1 + \tau_1 \frac{dT_1}{dt} \\ T_{g2} &= T_2 + \tau_2 \frac{dT_2}{dt} \end{aligned}\right\} \qquad (5)$$

where the subscripts 1 and 2 denote two thermocouples with different diameters d_1 and d_2.

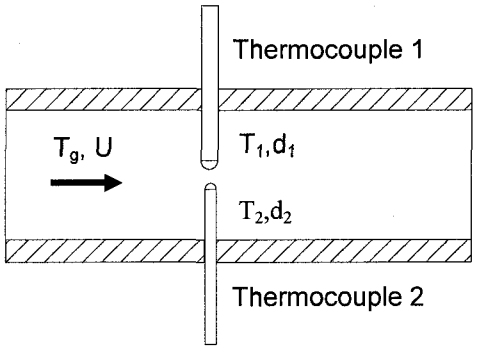

Figure 4-3 Illustration of the two thermocouples setup

Ideally, T_{g1} and T_{g2} should be identical because they are the gas temperature of the same location. In reality, there are differences between them. By minimizing the time average difference between the compensated temperatures T_{g1} and T_{g2} using the least squares method, the mean time constants, $\overline{\tau_1}$ and $\overline{\tau_2}$ can be estimated [30]. The time averaged difference between T_{g1} and T_{g2} can be expressed as:

$$e = \frac{1}{N}\sum_{i=1}^{N}(T_{g2}^{i} - T_{g1}^{i})^2 \tag{6}$$

where N is the number of samples per thermocouple and the superscript i denotes the sample at the time $i\Delta t$. If $\sum$ is used to abbreviate $(1/N)\sum_{i=1}^{N}$, and the definitions of $\Delta T_{21} = T_2 - T_1$, $G_1 = dT_1/dt$ and $G_2 = dT_2/dt$ are used, then

$$\begin{aligned} e = {} & \sum(\Delta T_{21})^2 + \overline{\tau_1}^2(\sum G_1^2) + \overline{\tau_2}^2(\sum G_2^2) \\ & - 2\overline{\tau_1}(\sum G_1 \Delta T_{21}) + 2\overline{\tau_2}(\sum G_2 \Delta T_{21}) \\ & - 2\overline{\tau_1}\,\overline{\tau_2}(\sum G_1 G_2) \end{aligned} \tag{7}$$

From Equation (7), with the conditions expressed in Equation (8), the time constant $\overline{\tau_1}$ and $\overline{\tau_2}$ can be obtained, as shown in Equation (9), to minimize e:

$$\left.\begin{aligned}\frac{\partial e}{\partial \overline{\tau_1}} &= 0 \\ \frac{\partial e}{\partial \overline{\tau_2}} &= 0\end{aligned}\right\} \tag{8}$$

$$\left.\begin{aligned}\overline{\tau_1} &= \frac{(\sum G_2^{\,2})(\sum G_1 \Delta T_{21}) - (\sum G_1 G_2)(\sum G_2 \Delta T_{21})}{(\sum G_1^{\,2})(\sum G_2^{\,2}) - (\sum G_1 G_2)^2} \\ \overline{\tau_2} &= \frac{(\sum G_1 G_2)(\sum G_1 \Delta T_{21}) - (\sum G_1^{\,2})(\sum G_2 \Delta T_{21})}{(\sum G_1^{\,2})(\sum G_2^{\,2}) - (\sum G_1 G_2)^2}\end{aligned}\right\} \tag{9}$$

By substituting $\overline{\tau_1}$ and $\overline{\tau_2}$ into Equation (5), the estimation of the exhaust gas temperatures T_{g1} and T_{g2} can be obtained.

4.2.2. Validation Experiments and Preliminary Results

To verify the temperature response model and to investigate the optimal combinations of thermocouples with different diameters, five type-K thermocouples were mounted in a radial configuration in the exhaust pipe of a Yanmar NFD170 single cylinder diesel engine, perpendicular to the flow field as shown in Figure 4-4. The five thermocouples included two 1/16" diameter (labeled as 1/16" A and 1/16" B respectively), one 1/8" diameter (1/8" A), one industrial 1/8" diameter (1/8" T) sheathed thermocouple, and one 0.005" diameter (0.005") bare wire thermocouple. The 1/16" A and 1/16" B were

identical thermocouples. Although 1/8" A and 1/8" T had the same bead size (1/8"), the diameter of the probe of 1/8" T was 1/4", while that of 1/8" A was 1/8".

The 0.005" bare wire thermocouple had a time constant of approximately 0.08 second in a 18.3m/s air flow for a temperature change between 38°C and 427°C [9]. Since the exhaust gas velocity was in the same range during the experiments in this study, the reading of the 0.005" thermocouple could be used to estimate the real-time exhaust gas temperature with acceptable accuracy. For this research, the reading of the 0.005" thermocouple was used to represent the real exhaust gas temperature.

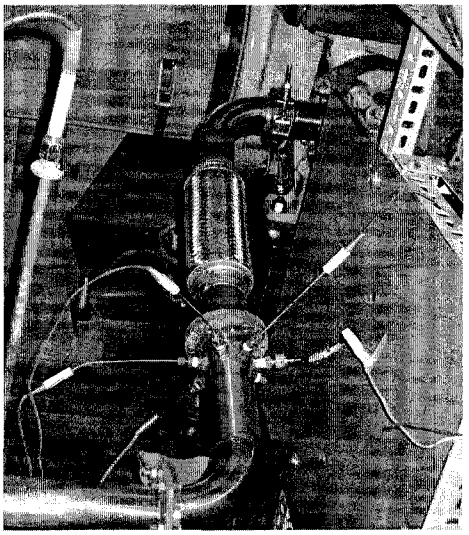

Figure 4-4 Experimental setup of the thermocouples

Engine tests were performed to generate significant temperature fluctuations in the exhaust stream and to use the temperature data to validate the model. All the thermocouple signals were collected at 100Hz sampling rate by using the data acquisition system introduced previously (see 3.1.2 for details). In the first test condition, the Yanmar

engine was operated with the dynamometer controller locked at 1820 rpm to represent the high exhaust flow rate conditions, while the fuel flow to the engine was changed transiently to generate the temperature fluctuations in the exhaust stream. In the second condition, the engine speed was reduced to 800 rpm to represent the low exhaust flow rate conditions and the fuel flow was again varied to produce the temperature fluctuations in the exhaust stream. Figures 4-5 and 4-6 show the temperature responses of the five thermocouples with different diameters during the test condition 1 and 2 respectively. Figures 4-7 and 4-8 are the enlarged parts of the temperature measurements with the 1/16"A, 1/8"A and 0.005" thermocouples.

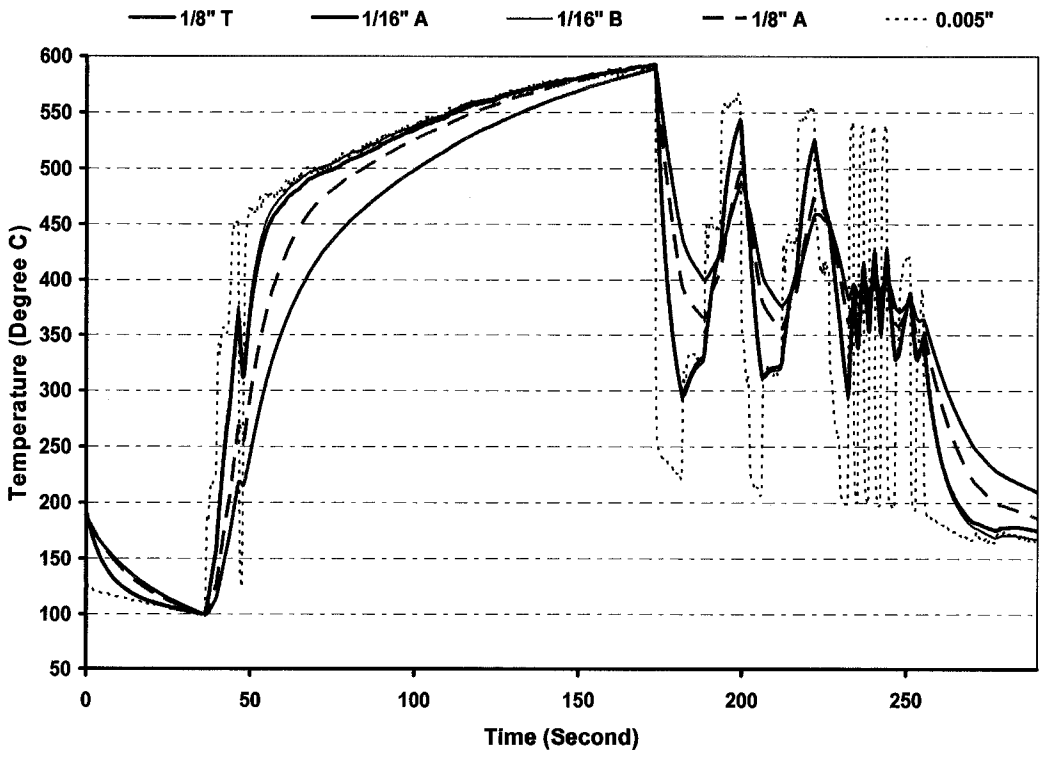

Figure 4-5 Temperature measurements under the test condition 1

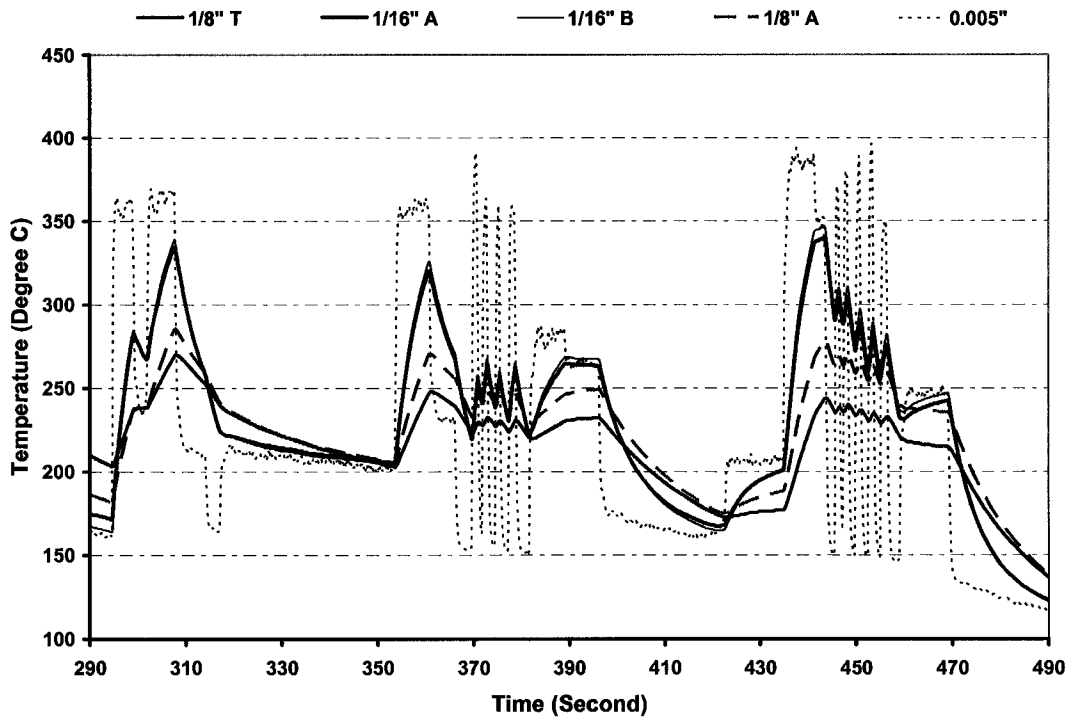

Figure 4-6 Temperature measurements under the test condition 2

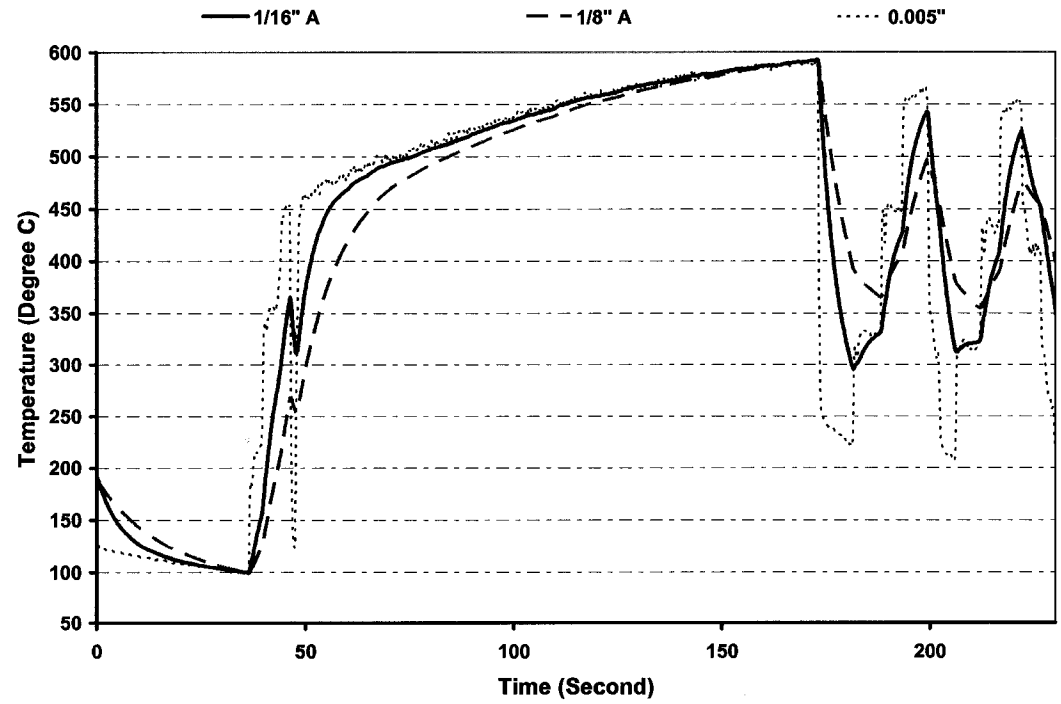

Figure 4-7 Enlarged temperature measurements under the test condition 1

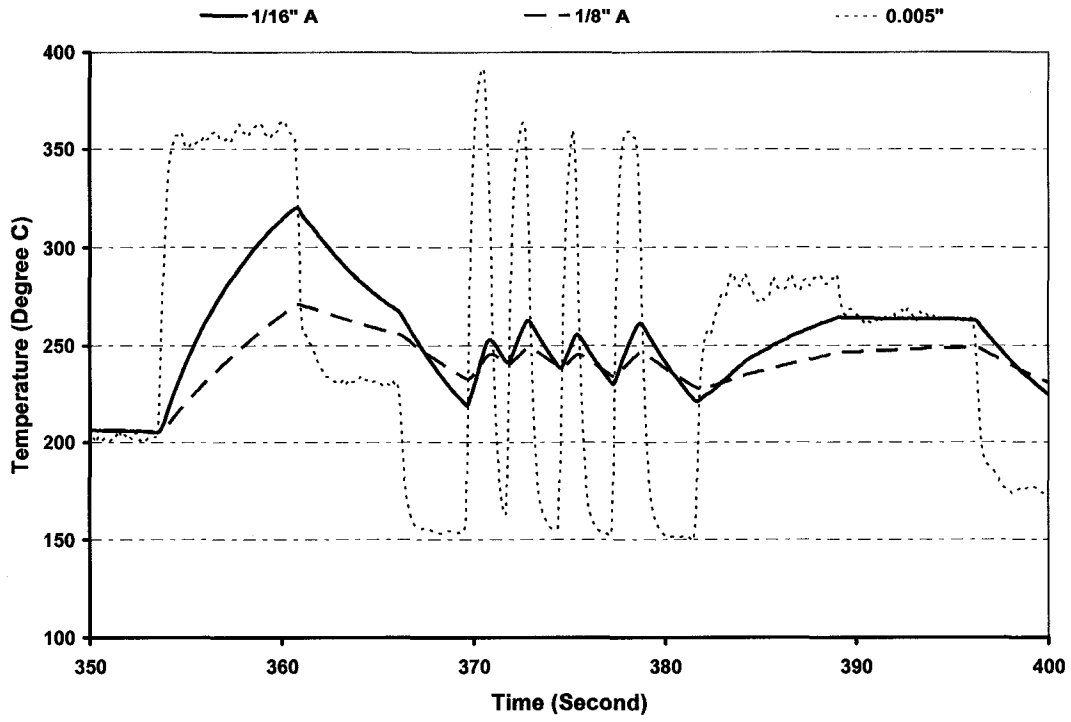

Figure 4-8 Enlarged temperature measurements under the test condition 2

The temperature response model was programmed in C language to calculate the compensated transient temperature and time constants of the two thermocouples offline based on the readings from the same two thermocouples. To calculate the $G_1 = dT_1 / dt$ and $G_2 = dT_2 / dt$, various combinations of the order of polynomial curve-fittings and the number of data points were inspected. The preliminary study showed that the linear curve-fitting using the data within the ±0.5 s neighborhood of the current data point could give satisfactory results. Therefore, the method was employed in the program to determine the G_1 and G_2.

Various combinations of the readings from two different thermocouples, such as 1/16" A with 1/8" A and 1/16" A with 1/16" B, were applied to estimate the compensated temperatures and time constants of the thermocouples under test condition 1 and 2. The time constant results under different combinations and conditions are summarized in Table 4-1. The results indicated that when two thermocouples with small diameter ratio were combined, this algorithm could not give reasonable results. For instance, when 1/16" A was combined with 1/16"B, the calculated time constant of 1/16" A was 1.4s for condition 1 and 0.8s for condition 2, which did not agree with the reality. However, if two thermocouples with higher diameter difference were used together, the calculated time constants results were reasonable.

Table 4-1 Summary of the time constants results

Test condition	Thermocouple B →	1/16"A	1/16"B	1/8"A	1/8"T
	Thermocouple A ↓	Time constant of thermocouple A when combined with thermocouple B (Second)			
1 (1820rpm)	1/16"A	--	1.4	3.7	3.2
	1/16"B	1.3	--	3.7	3.1
	1/8"A	8.7	9.0	--	6.3
	1/8"T	12.8	13.1	10.7	--
2 (800rpm)	1/16"A	--	0.8	4.9	3.2
	1/16"B	0.7	--	4.7	3.0
	1/8"A	11.5	11.6	--	1.9
	1/8"T	12.4	12.7	3.0	--

According to the manufacturer, the 1/16" sheathed thermocouple with ground junction has a time constant of approximately 4.0s in a 18.3m/s air flow for a temperature change between 38°C and 427°C [9]. When the 1/16" thermocouples were combined with 1/8" A, the calculated time constant was 3.7s for both 1/16" A and 1/16" B for test condition 1 with a flow rate of 14.5 g/s. These results indicated that the diameter ratio between the two thermocouples was critical to this method and a diameter ratio of two could give reasonable results.

It was also noticed that most time constants of the test condition 1 were smaller than that of the test condition 2 for the same thermocouple under the same combination. This is because the flow rate for test condition 1, 14.5 g/s, was higher than 6.4 g/s, the flow rate for the test condition 2. According to the heat transfer theory, the heat transfer rate by convection is higher in a higher flow rate field; thus, the time constant of the thermocouple is smaller.

With the readings for a proper combination of two thermocouples with the correct diameter ratio, such as 1/16" A and 1/8" A, the compensated temperature could be calculated by the C language program. Figure 4-9 is the comparison between the compensated temperatures by using 1/16" A and 1/8" A combination and the measured temperature from 0.005" thermocouple for test condition 1. The compensated temperature results of Figure 4-9 were in close agreement with the "real-time" value than the measured results of Figure 4-7. It was especially noticed that the compensated results

predicted the sudden temperature variations during the abrupt fuel-flow changes, for example, at t = 48s, 170s and 200s.

Figure 4-10 shows another comparison between the measured temperature from the fast-response thermocouple and the compensated temperatures from the two high-inertia thermocouples, 1/16" A and 1/8" A, for test condition 2. Again the compensated temperature results of Figure 4-10 were in reasonable agreement with the "real-time" value than the measured results of Figure 4-8, especially during the abrupt fuel-flow changes, such as those at t = 354s, 361s and 370s.

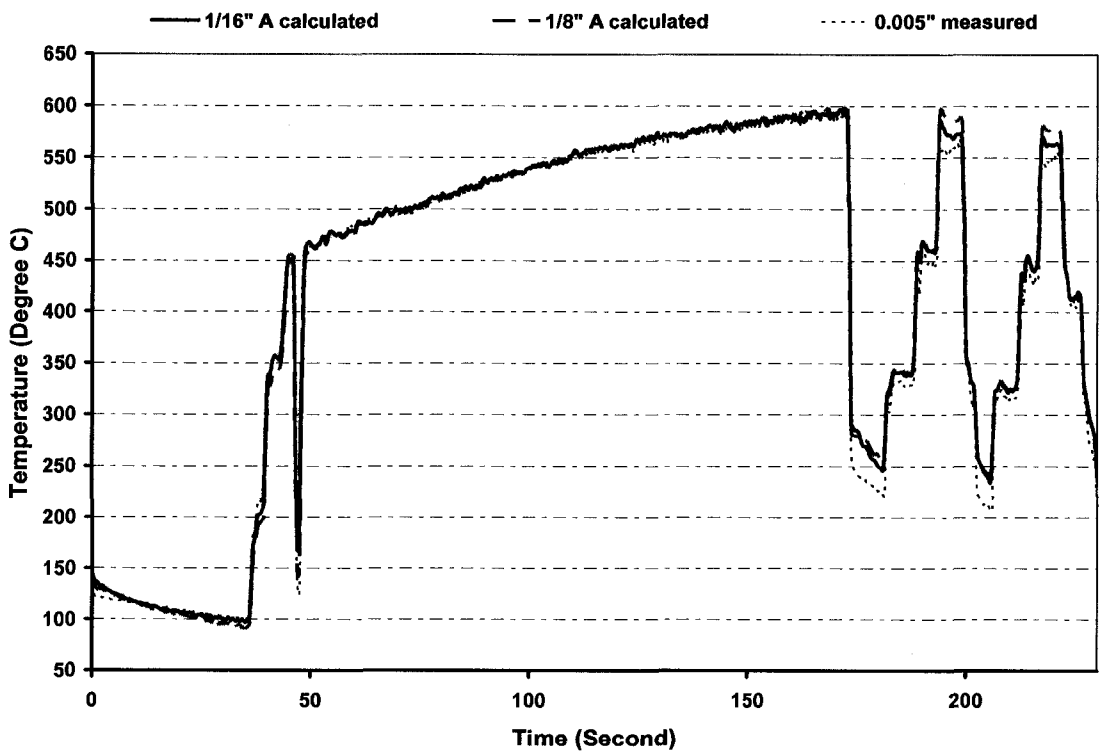

Figure 4-9 Comparison between the compensated temperatures by using 1/16" with 1/8" thermocouple combination and the measured temperature from 0.005" bare wire thermocouple for test condition 1

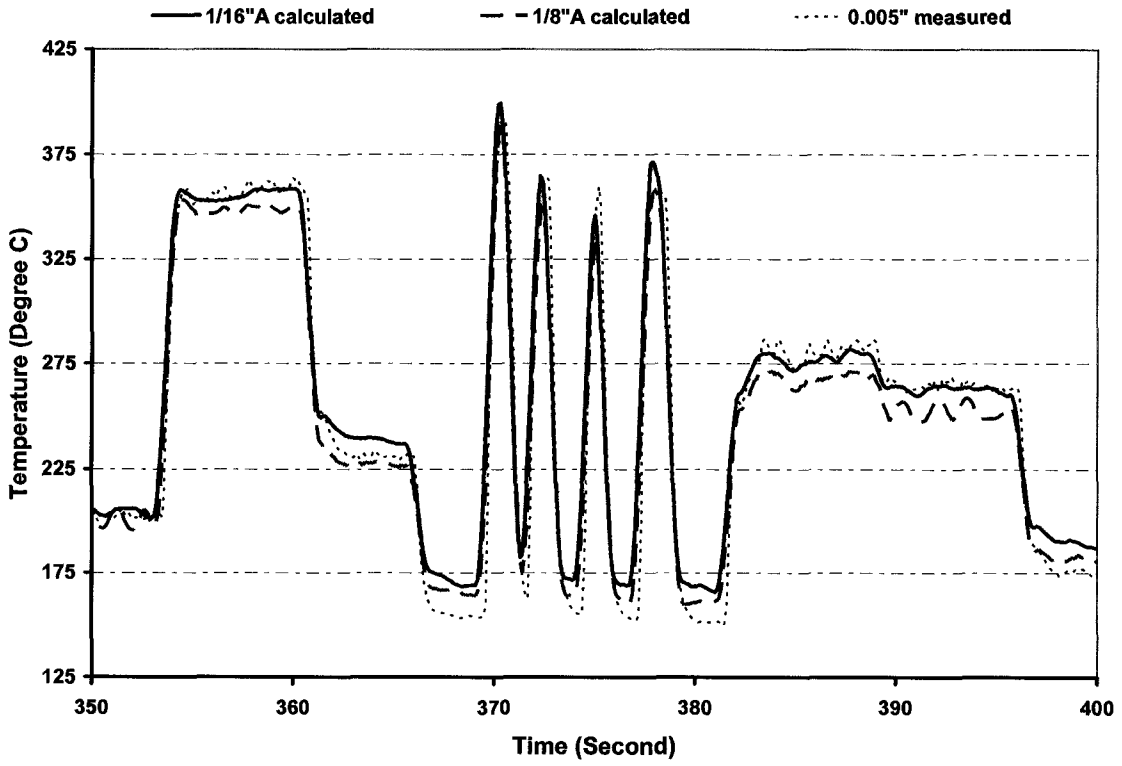

Figure 4-10 Comparison between the compensated temperatures by using 1/16" with 1/8" thermocouple combination and the measured temperature from 0.005" bare wire thermocouple for test condition 2

4.2.3. Real-Time Estimation of Transient Exhaust Temperature

After the validation of the temperature response model and the investigation of the appropriate thermocouple diameter ratio of the two thermocouples, the temperature response model was applied to estimate the transient exhaust temperature in real-time.

4.2.3.1. Real-Time Temperature Estimation Program

To estimate the transient exhaust temperature in real-time, the temperature response model was implemented into the multifunction data acquisition card NI PCI-6023E by

using LabVIEW. This LabVIEW program was capable of calculating the time constants of the two thermocouples in real-time and hence calculating the compensated transient exhaust temperature based on the readings of two thermocouples, mounted at close proximity and with the proper diameter ratio. In addition, it could display the traces of the compensated exhaust temperature and readings of two thermocouples graphically, as well as in text in real-time. All the measured and calculated data, such as the thermocouple readings, compensated exhaust temperature, and the real-time time constants of the thermocouples, were saved in a spreadsheet file with a name assigned by the user.

A brief initial period was necessary to calculate the first set of values for the two time constants and the transient exhaust temperature. The length of this period was entered by the user, with the recommended value about 1.5 to 2 times of the larger time constant of two thermocouples. Within the initial period, the compensated temperature was calculated based on the initial time constants entered by the user. Again, the linear curve-fitting method using the data within the past 0.5 s neighborhood of the current data point was employed in the program to determine the $G_1 = dT_1 / dt$ and $G_2 = dT_2 / dt$. The front panel and the block diagram of the LabVIEW program are shown in Figure 4-11 and 4-12 respectively.

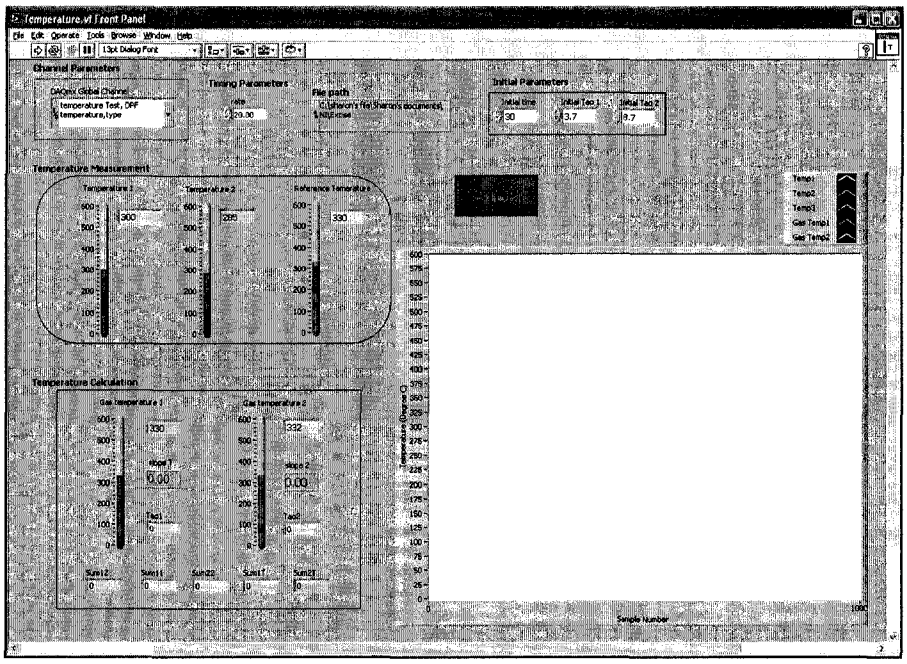

Figure 4-11 Front panel of the temperature real-time estimation program

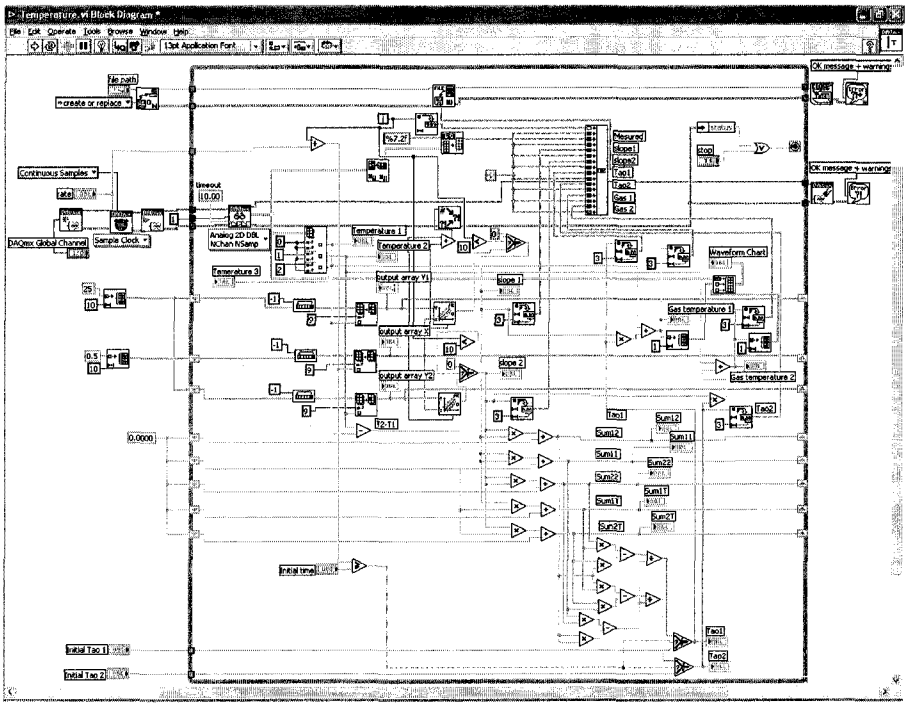

Figure 4-12 Block diagram of the temperature real-time estimation program

4.2.3.2. Engine Experiments and Preliminary Results

Engine experiments were performed to test the real-time temperature estimation program. Similar to the setup of validation experiments (see 4.2.2.), three type-K thermocouples were installed in a radical configuration in the exhaust pipe of the Yanmar NFD170 single cylinder diesel engine. The three thermocouples included one 1/16" diameter (1/16"), one 1/8" diameter (1/8") sheathed grounded thermocouple and one 0.005" diameter (0.005") bare wire thermocouple. For the same reason mentioned in 4.2.2., the reading of the 0.005" bare wire thermocouple was used to represent the real exhaust gas temperature.

Similar to the validation experiments (see 4.2.2.), significant temperature fluctuations were generated in the exhaust stream during the engine tests. During the engine tests, the Yanmar engine was operated with the dynamometer controller locked at 1600 rpm, while the fuel flow to the engine was changed transiently to generate temperature fluctuations in the exhaust stream.

The real-time temperature estimation program was run on the NI PCI-6023E to collect all the thermocouple signals at 20Hz sampling rate, and to calculate the time constants and compensated transient exhaust temperature using signals from the two thermocouples (1/16" & 1/8" combination) at the same time. Figure 4-13 shows the temperature responses from all the three thermocouples during the engine test.

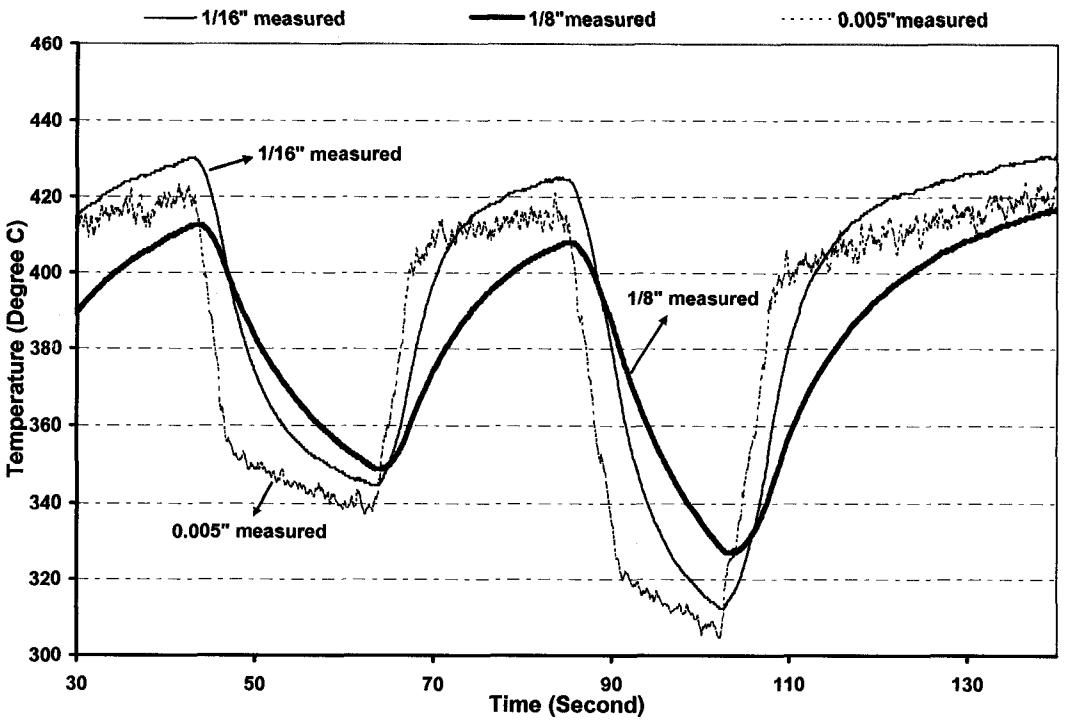

Figure 4-13 Temperature measurements from engine test

Figure 4-14 is the comparison between the real-time compensated temperatures by using the 1/16" and 1/8" combination and the measured temperature from the 0.005" thermocouple for the test condition. The compensated temperature results of Figure 4-14 were in close agreement with the "real-time" value than the measured results of Figure 4-13. It was especially noticed that the compensated results predicted the sudden temperature variations during the abrupt fuel-flow changes, such as those at t = 43s, 64s, 85s and 103s.

To compare the estimation of transient temperature with a single thermocouple to the estimation of transient temperature with two thermocouples, the readings of the 1/8"

thermocouple and the average time constant (11.3s) of the 1/8" thermocouple during engine test were applied to calculate the compensated exhaust temperature offline using the procedure for estimation of transient temperature with a single thermocouple. The comparison between the offline compensated temperature from a single 1/8" thermocouple, the real-time compensated temperature from a 1/8" thermocouple when combined with a 1/16" thermocouple, and the measured temperature from the 0.005" bare wire thermocouple for the test condition is illustrated in Figure 4-15. Although both the compensated temperature results can predict the sudden temperature changes, such as those at t=43s, 64s, 85s and 103s, the results from the 1/16" and 1/8" combination are in better agreement with the "real-time" temperature values.

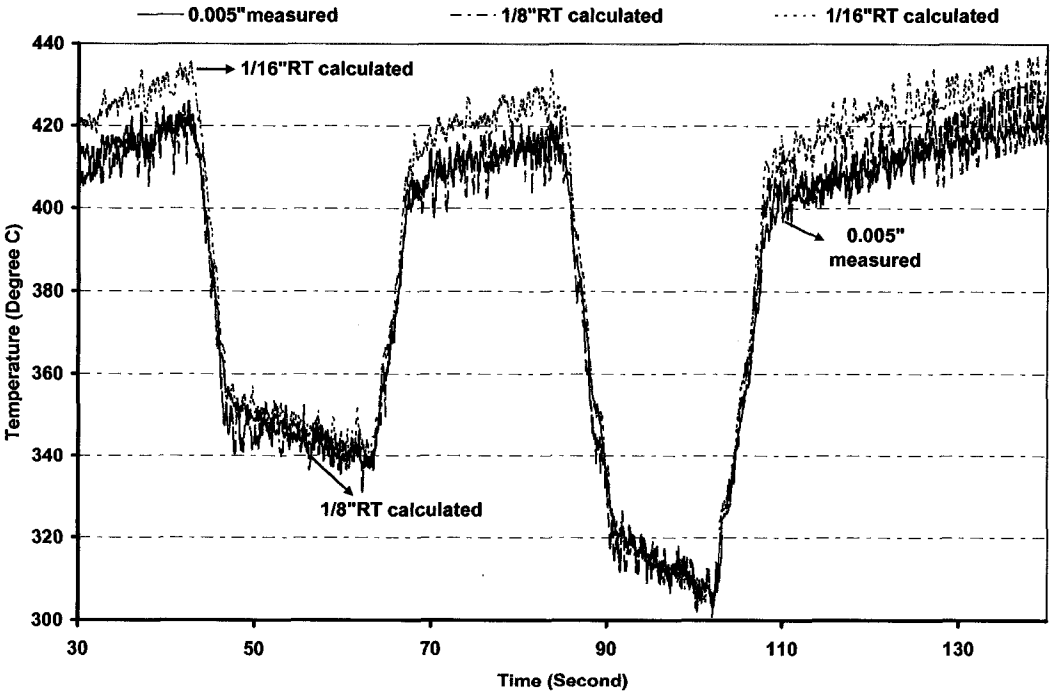

Figure 4-14 Comparison between the real-time compensated temperatures by using 1/16" and 1/8" thermocouple combination and the measured temperature from 0.005" bare wire thermocouple

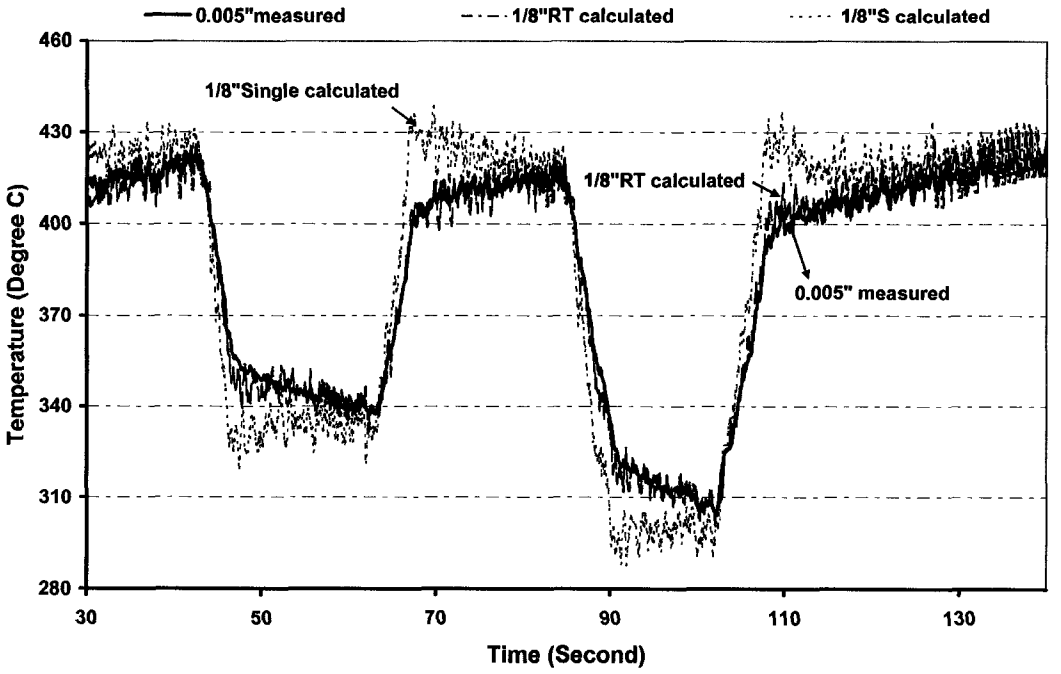

Figure 4-15 Comparison among the real-time compensated temperature by using 1/8" thermocouple readings when combined with 1/16" thermocouple, offline compensated temperature using single 1/8" thermocouple readings, and the measured temperature from 0.005" bare wire thermocouple

All the thermocouples used in this research were new thermocouples. Since the engine test duration was limited, some long term effects are not shown in Figure 4-15, such as that of the diameter variation of the thermocouple. After a long period of operation, a thermocouple probe inserted into the exhaust pipe near the exhaust valve of a diesel engine would be covered by a thick layer of soot, which will affect the response of the thermocouple to the fluctuating temperature and thus the value of the time constant. For the estimation of the transient exhaust temperature by using two thermocouples, such as the 1/16" and 1/8" combination, since the time constants are calculated in real-time, thus no additional error will be introduced. On the other hand, for the estimation of the transient exhaust temperature with a single thermocouple, such as 1/8", since the mean

time constant is fixed and the diameter change effect will not be taken into account, an additional error due to such effects as soot deposition will be brought into the temperature results.

Preliminary error analysis of the temperature response model showed that a significant error could occur by neglecting the conduction heat transfer. To reduce the conduction effect, proper thermal insulation of the experimental setup could be applied. This model relies on the quality of the data acquisition system, more attention should be paid to improve the data acquisition quality.

4.3. TRANSIENT MODEL OF AFTERTREATMENT

A transient model of aftertreatment was proposed to be included in the independent controller to present the simplified transient behavior of the diesel particulate filter (DPF) and the lean NOx trap (LNT). The basic concepts of the transient DPF and LNT models are presented below.

4.3.1. Transient DPF Model

In order to high lighten the importance of the aftertreatment control model, certain relative aspects of the modern aftertreatment strategy are described as follows. Since the mid-1980s, engine manufacturers have investigated devices to physically filter or trap particulates on the walls of a wall-flow honeycomb ceramic filter. The substrate of the

DPF is a ceramic honeycomb with half the channels closed at the inlet end and the other half of the channels closed at the exit end. The exhaust gases are forced to flow through the porous ceramic channel walls and exit at the adjoining channel, which is shown in Figure 4-16 [40]. The substrate is insulated by being wrapped with fiber materials and canned into a high quality, corrosion-resistant steel housing [2].

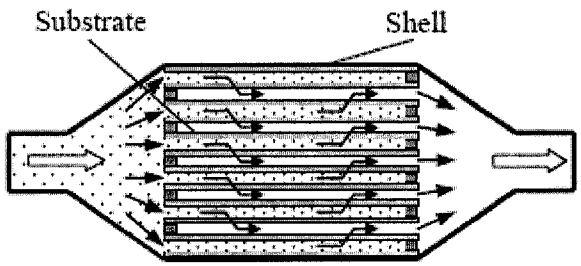

Figure 4-16 Schematic diagram of a DPF

While most commercial substrates show an excellent filtration efficiency, normally between 90% and 99%, each of these devices has a limited capacity to trap the particulates before the pressure in the exhaust system becomes very high and reduces the fuel efficiency excessively. The DPF then needs to be "cleaned off" by oxidizing the accumulated particulate matters (PM). This process is called as regeneration [2].

Without the help of a catalyst, the DPF needs a temperature around 550°C ~ 650°C to regenerate. However, this temperature range is too high for the modern diesel engines because the exhaust temperature of the modern diesel engines can be as low as 100°C and be less than 250°C most of the time for light-duty engines. To redesign and implement the DPF in order to fill the gap between these two temperature ranges while using less

supplemental energy is a major and active research topic. Many innovative strategies have been proposed, among which the active-flow control aftertreatment schemes are under investigation in the Clean Diesel Engine Laboratory, University of Windsor.

A DPF's performance could be affected by many parameters, such as the DPF structure, the material properties, the engine exhaust gas temperature, the exhaust gas flow rate, etc. The most important parameters are the engine exhaust temperature T_g and the pressure drop across the DPF, ΔP. Therefore, the output signals of the aftertreatment controller can be expressed as follows:

$$Fuel\ injection\ pattern = f_1(T_g, \Delta P) \tag{10}$$

$$Heater\ control\ pattern = f_2(T_g, \Delta P) \tag{11}$$

$$Exhaust\ valves\ control\ pattern = f_3(T_g, \Delta P) \tag{12}$$

The fuel injection pattern includes the frequency and the duty cycle of the output signal 1, which is a TTL square wave signal and is fed to the fuel injector drive circuit to control the fuel injector movement. The heater control pattern defines the on-set of an electrical heater; the exhaust valve control pattern has the information regarding the direction and the position of all the exhaust valves in the DPF setup.

Currently, Mr. Dong Wang, a PhD student of the author's group, is working to improve the regeneration performance of the DPF. The transient DPF model will be further developed based on his research achievements.

4.3.2. Transient LNT Model

The lean NO_x trap technology is one of the most promising methods to reduce the NO_x from the diesel engines. A LNT is a flow through catalyst bed that temporarily stores the engine out NO_x during lean burn operations. Before the NO_x absorbent becomes fully saturated, the engine operations are adjusted to produce a fuel rich exhaust. Under fuel rich conditions, the stored NO_x is released from the absorbent and subsequently reduced to N_2 over precious metal sites [3].

When a barium based absorbent is used, the exhaust NO is catalyzed to NO_2 by a Pt catalyst and the NO_2 is then stored as barium nitrate ($Ba(NO_3)_2$) during the lean operation, described by Equations 13 ~ 15 [3]. Under rich operation, the barium nitrate is decomposed and catalyzed to N_2 and O_2, as shown by Equations 16 and 17. Over long periods of operation, since there is sulfate in the diesel fuel and lubrication oil, barium sulfate ($BaSO_4$) is generated, which occupies the sites for the reversible NO_x absorption and desorption processes. A desulfurization process must be conducted at high temperature (650°C ~ 750°C) and fuel rich conditions.

$$NO + \frac{1}{2}O_2 \xrightarrow{Pt} NO_2 \tag{13}$$

$$BaCO_3 + 2NO + \frac{3}{2}O_2 \rightarrow Ba(NO_3)_2 + CO_2 \tag{14}$$

$$BaCO_3 + 2NO_2 + \frac{1}{2}O_2 \rightarrow Ba(NO_3)_2 + CO_2 \tag{15}$$

$$Ba(NO_3)_2 + 5CO \xrightarrow{Pt,Rh} BaO + 5CO_2 + N_2 \tag{16}$$

$$Ba(NO_3)_2 + 5H_2 \xrightarrow{Pt,Rh} BaO + 5H_2O + N_2 \quad (17)$$

The LNT operates on the same principle as a three-way catalyst converter (TWC), except that a higher amount of supplemental fuel is required to reduce the oxygen content of the raw exhaust gas and at a slower cycling rate (for instance 9 seconds lean followed by 1 second rich). The research of the active-flow control aftertreatment schemes of LNT is currently under investigation in the Clean Diesel Engine Laboratory and the research target is to realize the energy-efficient active control approach to improve the LNT performance, which includes the conversion efficiency, the fuel penalty, and the thermal stress.

Many parameters could affect the LNT's performance, such as the LNT structure, the material properties, the catalyst properties, the engine exhaust gas temperature, the exhaust gas flow rate, the exhaust NO_x concentration, etc. The most important parameters are the engine exhaust temperature T_g, the exhaust gas mass flow rate $\dot{m}$, the exhaust NO_x concentration $[NO_x]$ before the LNT, and the exhaust O_2 concentration $[O_2]$. Therefore, the output signals of the aftertreatment controller can be expressed as follows:

$$Fuel\ injection\ pattern = f_1(T_g, \dot{m}, [NO_x], [O_2]) \quad (18)$$

$$Heater\ control\ pattern = f_2(T_g, \dot{m}) \quad (19)$$

$$Exhaust\ valves\ control\ pattern = f_3(T_g, \dot{m}, [NO_x], [O_2]) \quad (20)$$

$$\text{Re}\,quirement\ to\ engine = f_4(T_g, \dot{m}, [NO_x], [O_2]) \quad (21)$$

The first three signals function similar to those for the DPF model, described in the previous section. The last signal will be sent to the engine to "request" for more favorable conditions for the LNT, such as a post injection.

Currently, Ms. Jun Zuo, a PhD student of the author's group, is conducting the research to improve the performance of the LNT with less supplemental energy. The transient LNT model will be further developed based on her research accomplishments.

4.4. DECISION-MAKING PROGRAM

The decision-making program, which is the software of the proposed independent aftertreatment controller, defined how the independent controller functions. It was a LabVIEW program running at the NI PCI-6023E DAQ board and consisted of the data acquisition, control algorithm and the signal output functions, as shown in Figure 4-17. In the data acquisition part, the program defined the data acquisition channels which were used to collect the signals from the sensors at the specific sampling rate and the specific sampling mode, in the sampling order according to the user's choice. In addition, how the signals were saved and displayed graphically and/or in text was also defined by the program.

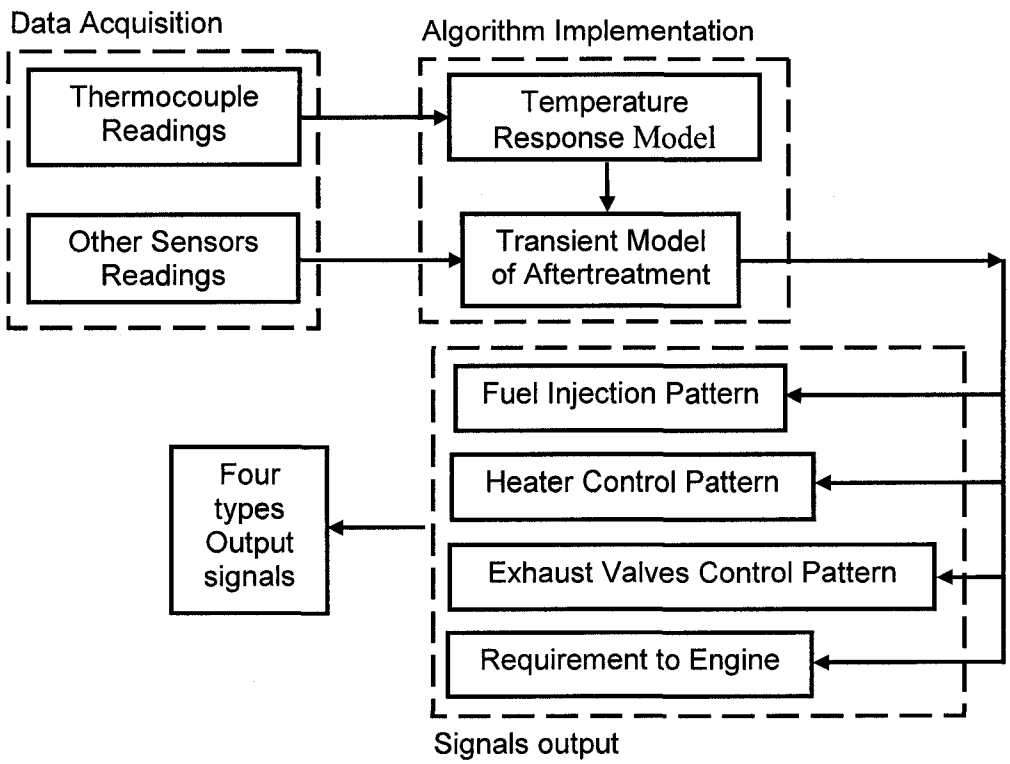

Figure 4-17 Decision-making program layout

The implementation of the temperature response model and the transient model of aftertreatment devices formed the algorithm implementation part, which was the major part of the decision-making program. The thermocouple readings were fed into the temperature response model to generate the compensated transient exhaust temperature which was in turn input into the transient model of the aftertreatment devices, while the other sensors' readings, such as the pressure transducers, were used by the transient model directly. The patterns of the four types of output signals, for instance, the frequency, the duty cycle and the pulse number of the fuel injection signal, would be

calculated by the transient model of the aftertreatment devices and output to the next part of the decision-making program, the signal output part.

In the signal output part of the decision-making program, the last part of the program, the four types of the output signals, such as the fuel injection, the heater control, the exhaust valves control and the requirement to the engine signals, would be generated according to the patterns calculated by the transient model of aftertreatment devices. The transient temperature determined from this research will help the implementation of overall control strategy.

5. CLOSED LOOP SYSTEMS

In this chapter, a very simple closed loop system is introduced briefly, followed by a detailed report of another closed loop system aimed at maintaining the temperature of the diesel aftertreatment device's substrate. The experimental setup and the preliminary test results of the latter system are presented.

5.1. SIMPLE CLOSED LOOP SYSTEM

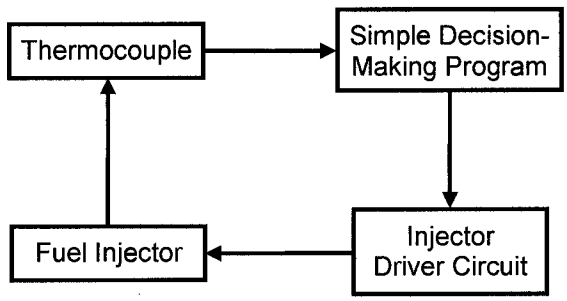

Figure 5-1 Simple closed loop system

In order to test and calibrate the primary components of the control system, a simple closed loop system which included a thermocouple, a simple decision-making program, the fuel injector driver circuit, and a gasoline fuel injector, was built. Based on the temperature reading obtained by a 1/16" diameter sheathed grounded thermocouple, the fuel injector injected water accordingly. The frequency and the duty cycle of the output TTL square wave signal were calculated by the simple decision- making program based on a dummy model to realize the objective of "the higher the temperature the faster and

larger the amount of water injection". Figure 5-1 illustrates the simple closed loop system, and Figure 5-2 shows the injector during water injection.

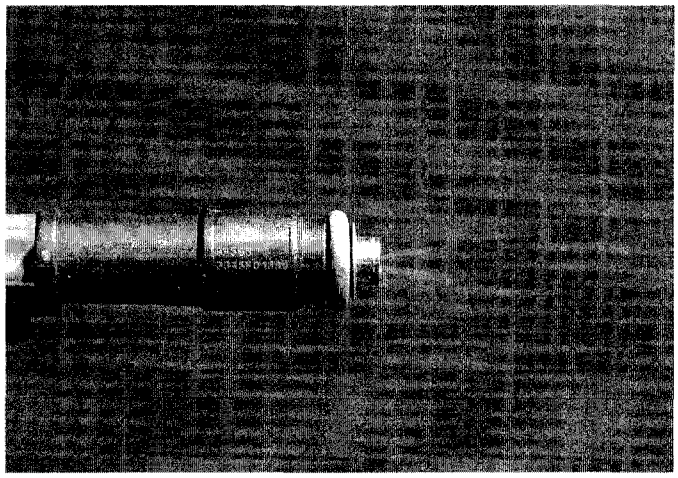

Figure 5-2 Water injection

5.2. CLOSED LOOP SYSTEM FOR SUBSTRATE TEMPERATURE CONTROL

5.2.1. Experimental System Setup

To control the temperature of the diesel aftertreatment device's substrate, a closed loop system was built to inject proper amount of supplemental diesel fuel into the aftertreatment system of the Yanmar NFD 170 single cylinder diesel engine. The schematic diagram of the system is illustrated in Figure 5-3, and Figure 5-4 is the picture of the experimental system. Eight type-K thermocouples, as summarized in Table 5-1, were placed in different positions inside the substrate of the aftertreatment device, and the engine exhaust pipe at the up stream and down stream of the aftertreatment device. All eight thermocouples were connected to the NI PCI-6023E multifunction data acquisition

(DAQ) board in the host PC through the NI SCXI signal conditioning system (see 3.1.2. for details). The TTL output signal of the PCI-6023E DAQ board was fed to the fuel injector driver circuit (see 3.2. for detail) and then the fuel injector to control its operation. The fuel injector and its setup introduced in section 3.4. were applied while the diesel fuel was supplied to the fuel injector at a pressure of 2 bar.

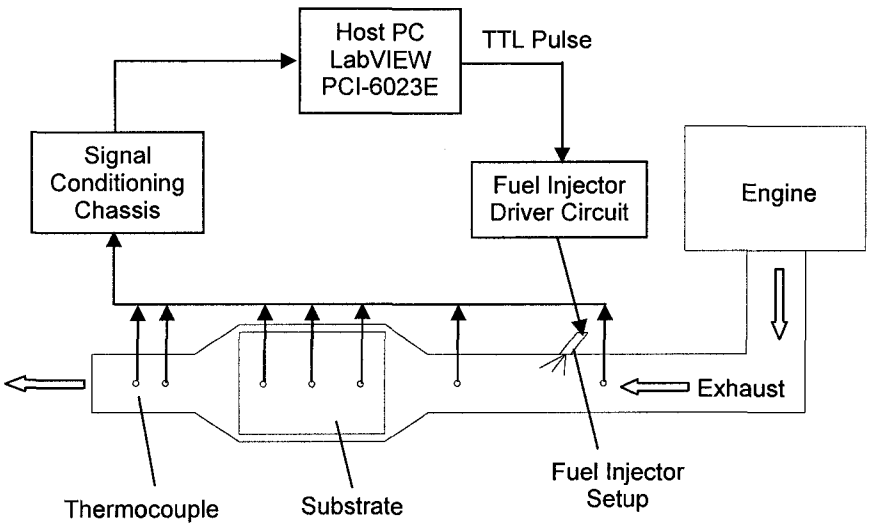

Figure 5-3 Schematic diagram of substrate temperature control system

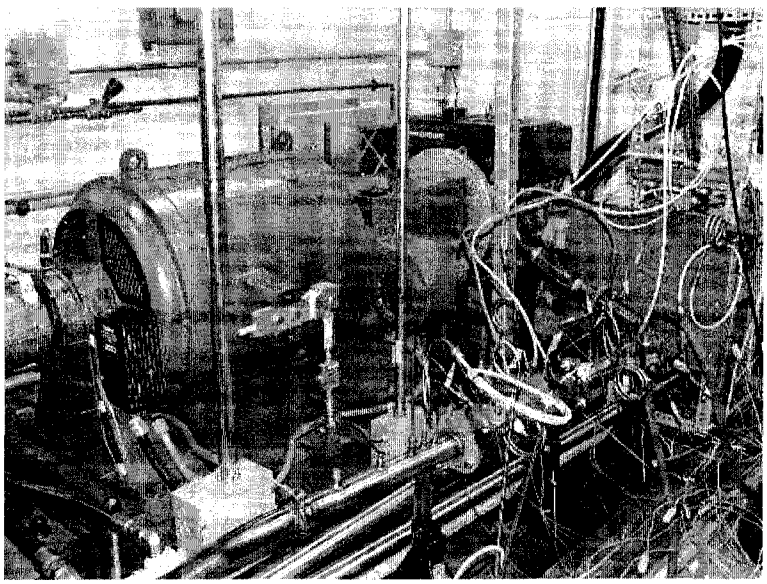

Figure 5-4 Substrate temperature control system

5.2.2. Decision-Making Programs and Preliminary Results

According to the function of its decision-making program, the substrate temperature control system can be operated manually or as an automatic system. In this section, both the manual and the automatic decision-making programs for the temperature control system are introduced, and the preliminary engine test results of both the manual and the automatic systems are presented.

Table 5-1 Summary of thermocouples used in substrate temperature control system

No.	Name	Description	Location
1	1/16"-1	Omega TJ36-CASS-116G-6 transition joint probe, grounded junction, junction and probe size 1/16"	Up stream of fuel injector, near engine exhaust port
2	1/8"-1	Omega TJ36-CASS-18G-6 transition joint probe, grounded junction, junction and probe size 1/8"	Up stream of fuel injector, away from engine exhaust port
3	1/16"-2	Omega TJ36-CASS-116G-6 transition joint probe, grounded junction, junction and probe size 1/16"	Down stream of fuel injector, up stream of substrate
4	1in	Omega TJ36-CASS-140G-6 transition joint probe, grounded junction, junction and probe size 1/40"	Inside the substrate, 1 inch from the inlet of the substrate
5	3in	Omega TJ36-CASS-140G-6 transition joint probe, grounded junction, junction and probe size 1/40"	Inside the substrate, 3 inches from the inlet of the substrate
6	5in	Omega TJ36-CASS-140G-6 transition joint probe, grounded junction, junction and probe size 1/40"	Inside the substrate, 5 inches from the substrate inlet
7	1/16"-3	Omega TJ36-CASS-116G-6 transition joint probe, grounded junction, junction and probe size 1/16"	Down stream of the substrate, near the substrate outlet
8	1/8"-2	Omega TJ36-CASS-18G-6 transition joint probe, grounded junction, junction and probe size 1/8"	Down stream of the substrate and 1/16"-3 thermocouple

5.2.2.1. Manual Substrate Temperature Control System

To try out the experimental setup of the substrate temperature control system and to find the basic range of the control parameters used in the automatic control decision-making program, the manual substrate temperature control system was tested first. The decision-making program of the manual control system generated the fuel injection TTL pulse output signals with the variable frequencies and duty cycles according to the real-time input by the operator using the front panel control. Figure 5-5 shows the front panel of the LabVIEW decision-making program of the manual control system.

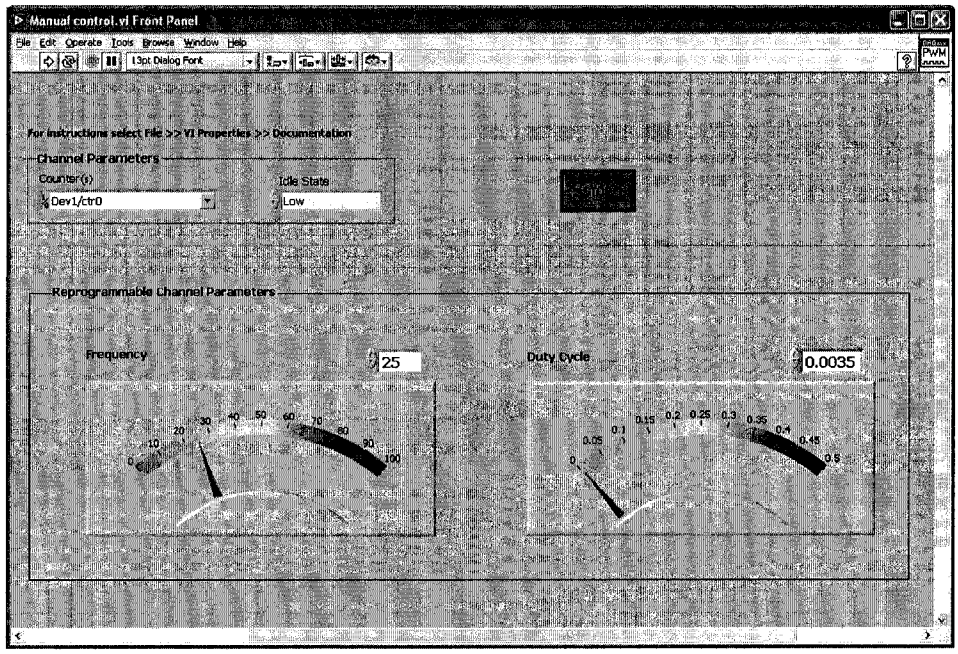

Figure 5-5 Front panel of the decision-making program of the manual substrate temperature control system

During the engine test, the Yanmar engine was operated with the dynamometer controller locked at 1500 rpm and the torque varying from 25 to 48 N·m. All the thermocouple signals were collected at a 10Hz sampling rate by using the data acquisition system and

displayed digitally and graphically on the monitor of the host PC. By observing the temperature display and considering the set point of the substrate temperature, which was 600°C in this experiment, the operator adjusted the frequency and the duty cycle of the fuel injection TTL pulse accordingly, to inject the proper amount of diesel fuel into the aftertreatment system and to maintain the temperature of the substrate around 600°C. The temperature measurements during the engine test are shown in Figure 5-6. At t= 500s, the engine torque changed from 48 N·m to 25 N·m and exhaust gas temperature decreased from 365°C to 220°C. By injecting diesel fuel at 25 Hz with the duty cycle varying between 0.032 and 0.035, the temperature of the substrate was retained near 600°C until the fuel injection stopped at 1130s.

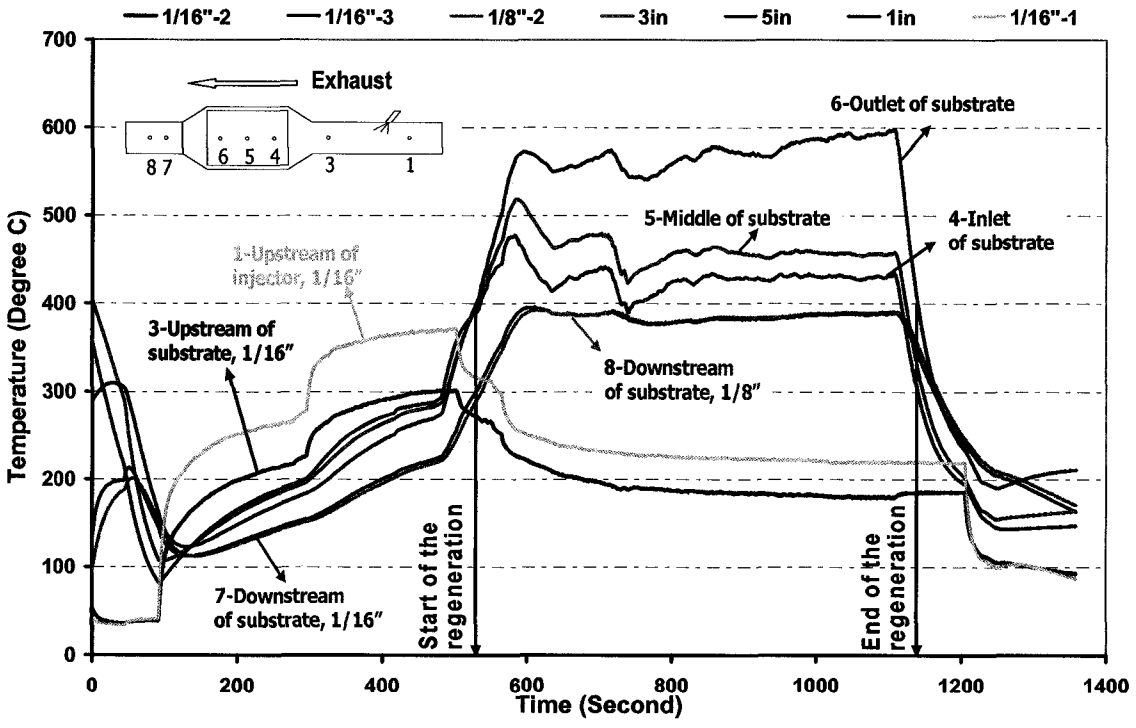

Figure 5-6 Temperature measurements during the engine test for the manual substrate temperature control system

5.2.2.2. Automatic Substrate Temperature Control System

Unlike that of the manual substrate temperature control system, the frequencies and the duty cycles of the fuel injection TTL pulse of the automatic substrate temperature control system were calculated in real-time by the decision-making program based on the thermocouple readings and the substrate temperature set point. Figure 5-7 shows the front panel of the LabVIEW decision-making program of the automatic substrate temperature control system. The maximum current temperature reading obtained from the thermocouples located inside the substrate, such as thermocouple 1in, 3in and 5in (see Table 5-1), was compared with the substrate temperature set point and the difference was applied to calculate the duty cycle of the next fuel injection TTL pulse.

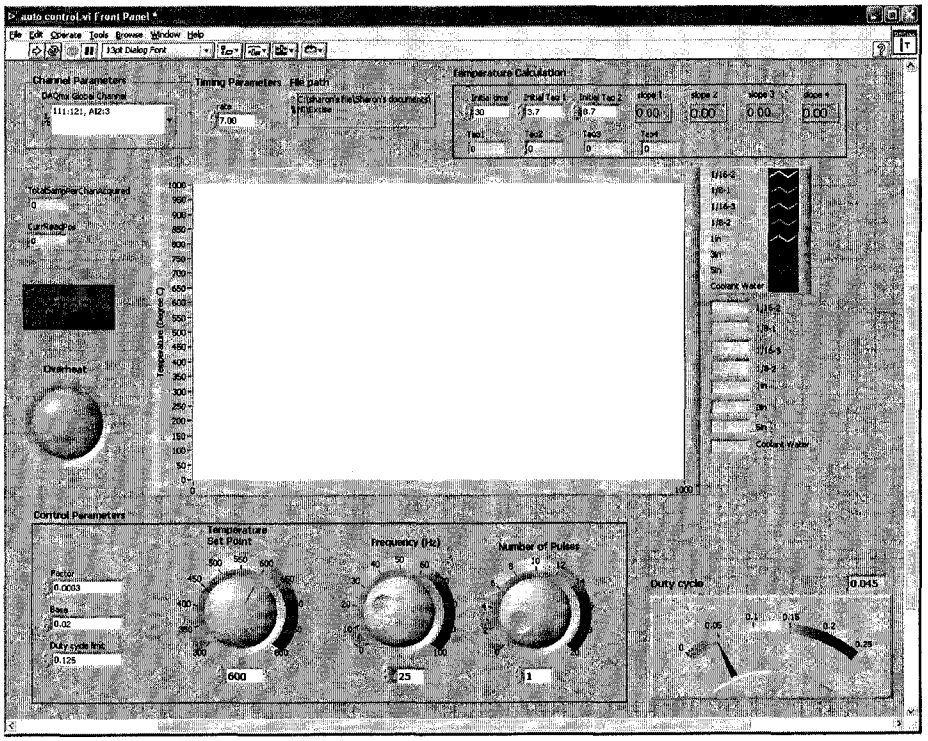

Figure 5-7 Front panel of the decision-making program of the automatic substrate temperature control system

During the validating engine experiment of the automatic substrate temperature control system, the Yanmar engine was operated with the dynamometer controller locked at 1700 rpm and the fuel flow to the engine was changed transiently to generate temperature fluctuations in the exhaust stream. The decision-making program was running at 7Hz at the PCI-6023E DAQ board to collect the thermocouple signals and to implement the algorithm to generate the fuel injection TTL pulse output signal. The frequency of the TTL pulse was fixed at 25Hz while the duty cycle of the TTL pulse was calculated in real-time. The temperature measurements for the test are shown in Figure 5-8. Since the diesel engine exhaust temperature is directly proportional to the engine load, therefore, from t = 630s to 1050s, when the engine load was varied extensively, there was a corresponding change in the engine exhaust gas temperature. During this time period, the highest substrate temperature, observed at 1" from the substrate outlet, was maintained around 570°C when the set point of the substrate temperature was 600°C by referencing the maximum of the three temperatures getting from the substrate.

Figures 5-9 and 5-10 illustrate the different intended control signals and the fuel injection TTL pulse, during different time periods of the engine test. In Figure 5-9, when the highest substrate temperature, that is, the temperature reading from the 5in thermocouple at this time period, was 539°C, the high time of each intended fuel injection TTL pulse was 4.2 ms, the equivalent duty cycle was 0.1061, and the flow rate of the diesel fuel injected into the aftertreatment system was 0.071 g/s. However, when the highest substrate temperature was 572°C, as shown in Figure 5-10, the high time of each intended

fuel injection TTL pulse was reduced to 2.2 ms, the equivalent duty cycle was 0.0558 and the flow rate of the diesel fuel injected into the aftertreatment system was 0.037 g/s, which meant that less diesel fuel was injected into the aftertreatment system.

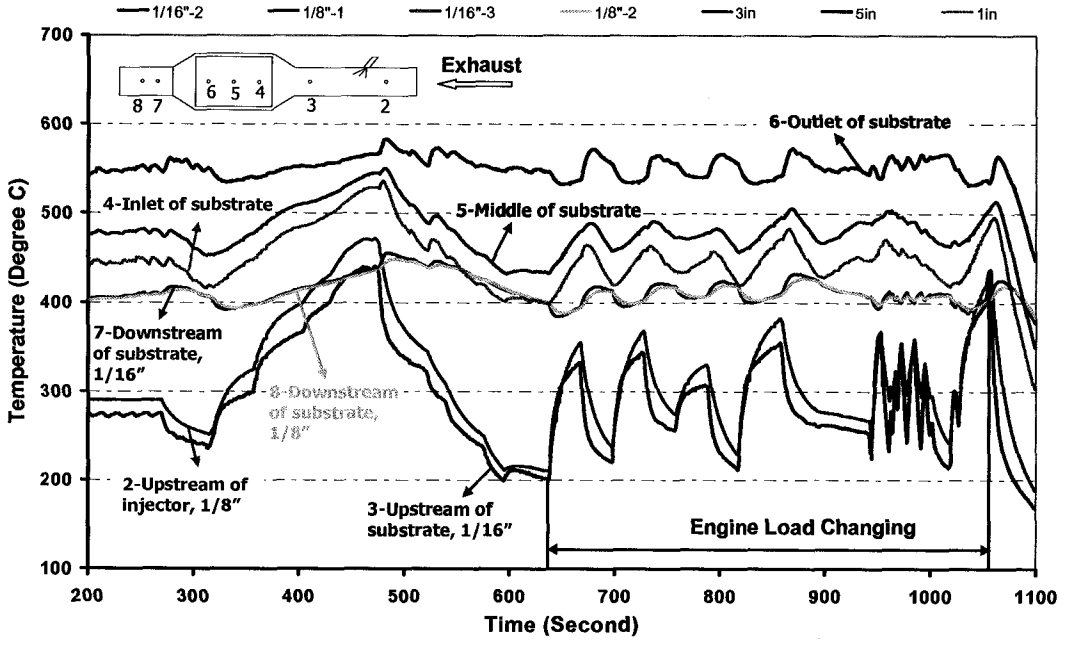

Figure 5-8 Temperature measurements during the engine test for the automatic substrate temperature control system

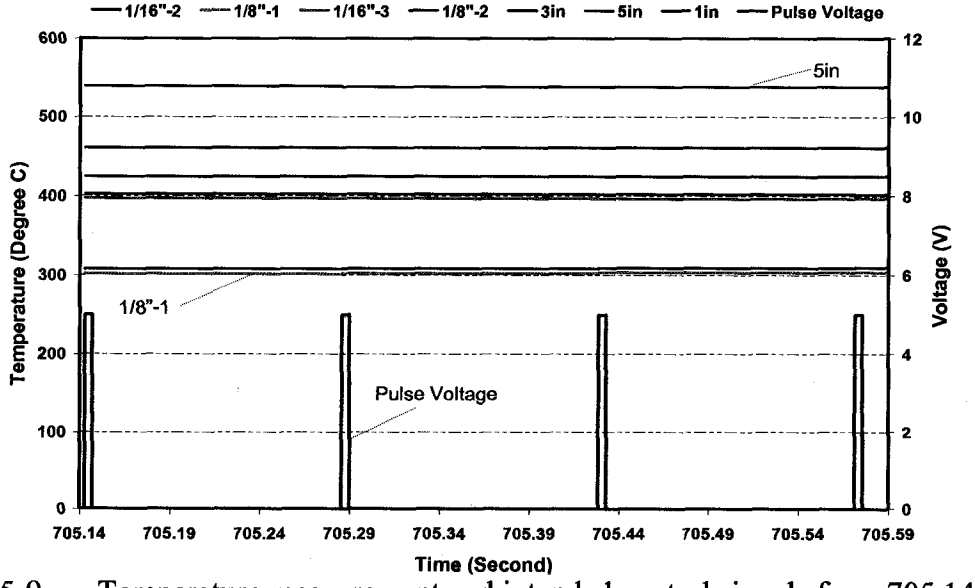

Figure 5-9 Temperature measurement and intended control signals from 705.14s to 705.59s

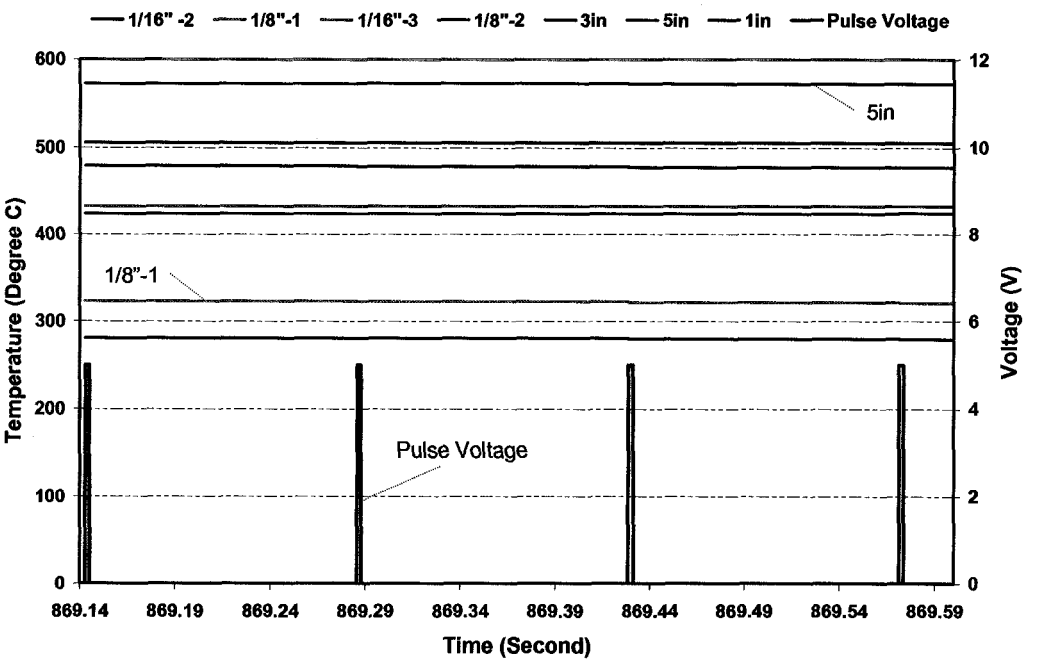

Figure 5-10 Temperature measurement and intended control signals from 869.14s to 869.59s

6. CONCLUSIONS AND RECOMMENDATIONS

6.1. CONCLUSIONS

To meet the increasingly stringent emission regulations and to remain the high energy efficiency of the diesel engines, an independent controller was proposed to perform real-time diagnosis and modeling based control for diesel aftertreatment devices, such as the diesel particulate filter and the lean NO_x trap. The experimental setup for the independent controller was proposed and the majority of the setup was finished, including that of the data acquisition system, the fuel injector driver circuit, the fuel injector and some sensors, such as the thermocouples, the mass air flow meter, the fuel flow meter and the rotary encoder. The exhaust flow control valves were acquired and tested. This research has produced the following conclusions:

1. A closed loop system was proposed to realize the objective of this research, to reduce the amount of the supplemental energy consumption through an independent control of the aftertreatment temperature, the exhaust flow and the excess air/fuel ratios λ.
2. A temperature response model that uses the temperature data obtained with two high-inertia thermocouples of proper diameter ratio to estimate the diesel engine transient exhaust gas temperature was developed.
3. Engine tests were performed to validate the temperature response model. It was discovered that the diameter ratio of the two thermocouples is critical to the

temperature response model. Based on the experimental data and analysis, the diameter ratio of 2 is recommended.

4. The sizes of the two thermocouple beads are not needed to determine the time constants of the thermocouples. Therefore, the variation of the size of the thermocouple over a long period of operation would not bring in addition errors to the estimation of the transient exhaust temperature.

5. The temperature response model was implemented into the multifunction data acquisition card NI PCI-6023E by using LabVIEW to estimate the transient exhaust temperature in real time. Engine tests were carried out to verify the real-time temperature estimation program. The real-time compensated temperature results were in good agreement with the temperature measurements recorded simultaneously by a third thermocouple of high sensitivity approximating the real-time value.

6. Simplified transient models for the diesel particulate filter and the lean NO_x trap were proposed.

7. The layout of the decision-making program of the independent controller was proposed. The program consisted of the data acquisition part, the algorithm implementation part and the signal output part.

8. A simple closed loop system was built. The simple decision-making program was based on a dummy model to realize the objective of "the higher the temperature the faster and larger the amount of water injection".

9. A closed loop system was built to control the temperature of the substrate of the aftertreatment device at the set point by injecting the proper amount of diesel fuel into the aftertreatment system. Depending on the properties of the decision-making programs, the substrate temperature control system can either be a manual or an automatic system.

10. The manual substrate temperature control system was developed and tested by the engine experiments. In the decision-making program of this system, the frequency and the duty cycle of the fuel injection TTL pulse were manually input by the operator. The temperature measurement of the engine test indicated that the temperature of the aftertreatment device's substrate was successfully maintained at the set point, of 550°C ~600°C, while the exhaust temperature of the engine changed.

11. The automatic substrate temperature control system was developed and validated by the engine tests. In the decision-making program of this system, the duty cycle of the fuel injection TTL pulse was calculated in real-time based on the difference between the maximum substrate temperature measurement and the set point, 600°C. The temperature measurement of the engine test indicated that the temperature of the aftertreatment device's substrate was successfully maintained at 570°C, while the exhaust temperature of the engine fluctuated.

6.2. RECOMMENDATIONS

The following works are recommended to improve the proposed independent controller for the diesel aftertreatment:

1. Improve the development of the transient model of the aftertreatment devices, such as the DPF and the LNT, and implement the model into the decision-making program.
2. Transfer the decision-making program from the NI PCI-6023E DAQ board to an NI PXI Real-Time controller. With the LabVIEW Real-Time Module and the stand-alone Real-Time controller, the execution of the decision-making program will be fast and, more importantly, deterministic and robust.
3. Complete the experimental setup, such as placing more sensors into the aftertreatment system and the engine, setting up the exhaust flow control valves and the electrical heater, and developing the driver circuits for the electrical heater if the circuits are needed.

REFERENCES

1. M. Zheng, class notes of "Fundamentals of Clean Engine Technology", University of Windsor, 2003.

2. J. B. Heywood, Internal Combustion Engine Fundamentals, McGraw-Hill Inc., ISBN 0-07-028637-X, 1988.

3. M. Zheng, G. T. Reader, Energy efficiency analyses of active flow aftertreatment systems for lean burn internal combustion engines, Energy Conversion and Management, v 45, n 15-16, September 2004, p 2473–2493.

4. M. Zheng, E. Mirosh, *et al*, Development of a compact reverse-flow catalytic converter for Diesel dual fuel LEV, SAE (Society of Automotive Engineers) Paper 1999-01-3558, 1999.

5. B. Liu, R. E. Hayes, M. D. Checkel, M. Zheng, E. Mirosh, Reverse flow catalytic converter for a natural gas / Diesel dual fuel engine, Chemical Engineering Science, v 56, n 8, May 2001, p 2641–2658.

6. V. O. Strots, G. A. Bunimovich, Y. S. Matros, M. Zheng, E. Mirosh, Novel catalytic converter for natural gas powered Diesel engines, SAE 980194, 1998.

7. M. Zheng, E. Mirosh, *et al*, A novel reverse-flow catalytic converter operated on an ISUZU-6HH1 Diesel dual fuel engine, 1999 ASME (American Society of Mechanical Engineers)-IEC Fall Technical Conference Proceedings, 1999.

8. J. Benajes, S. Molina and J. M. Garcia, Influence of pre- and post-injection on the performance and pollutant emissions in a HD diesel engine, SAE Paper 2001-01-0526, 2001.

9. OMEGA Engineering Inc., The Temperature Handbook, 21st Century™, Second Edition, 2000.

10. Robert Bosch GmbH, Technical customer information, 2000.

11. ONO SOKKI Home > English > Products > Automotive Industry (Instruments) > Volumetric Type Fuel Flow Detector FP Series, http://www.onosokki.co.jp/English/hp_e/products/keisoku/automotive/fp_df.html, accessed August 2004.

12. ONO SOKKI Home > English > Products > Automotive Industry (Instruments) > Digital Flow Meter DF-210A/211A, http://www.onosokki.co.jp/English/hp_e/products/keisoku/automotive/df210a.html, accessed August 2004.

13. Gurley Precision Instruments Home > Optical Encoders > Rotary Incremental Encoders > Models 9125 and 9225 rotary incremental encoders > 9X25S SERIES DATASHEET, http://www.gpi-encoders.com/PDF/925.pdf, accessed February 2004.

14. National Instruments Home > Products & Services > Data Acquisition (DAQ) > Multifunction Data Acquisition (DAQ) > E Series Multifunction DAQ > 12-Bit, 200 kS/s, Low-Cost > NI PCI-6023E, http://sine.ni.com/apps/we/nioc.vp?cid=10967&lang=US, accessed June 2003.

15. National Instruments Home > Products & Services > Signal Conditioning > SCXI High-Performance Signal Conditioning > Analog Input Modules > Thermocouples > NI SCXI-1102, http://sine.ni.com/apps/we/nioc.vp?cid=1654&lang=US, accessed November 2003.

16. National Semiconductor Home > Products > Automotive > Peripheral Drivers > LM1949 > Datasheet, http://www.national.com/ds/LM/LM1949.pdf, accessed October 2003

17. SIEMENS VDO Automotive, Smart ACV generic specification, 2003.

18. Park Hannifin Corporation, Gold Ring solenoid valve installation and maintenance instructions, 1992.

19. National Instruments, Measurement and automation catalog 2005, 2005.

20. R. J. Moffat, How to specify thermocouple response, Instrument Society of America - Journal, v 4, n 6, June 1957, p 219-223.

21. Y. A. Çengel, Introduction to thermodynamics and heat transfer, McGraw-Hill Companies, Inc., ISBN 0-07-011498-6, 1997.

22. A. Ballantyne, J. B. Moss, Fine wire thermocouple measurements of fluctuating temperature, Combustion Science and Technology, v 17, 1977, p 63-72.

23. K. C. Hopkins, J.C. Larue, G. S. Samuelsen, Effect of mean and variable time constant on compensated thermocouple measurements, NATO Advanced Study Instituteon Instrumentation for Combustion and Flow in Engines, Dordrecht: Kluwer, 1988.

24. R. Talby, F. Anselmet, L. Fulachier, Temperature fluctuation measurement with fine thermocouples, Experiments in Fluids, v 9, n 1-2, April 1990, p 115-118.

25. S. J. Park, S. T. Ro, A new method for measuring time constants of a thermocouple wire in varying flow states, Experiments in Fluids, v 21, n 5, September 1996, p 380-386.

26. P. C. Miles, F. C. Gouldin, Determination of the time constant of fine-wire thermocouples for compensated temperature measurements in premixed turbulent flames, Combustion Science and Technology, v 89, 1993, p 181-199.

27. W. C. Strahle, M. Muthukrishnan, Thermocouple time constant measurement by cross power spectra, AIAA (American Institute of Aeronautics and Astronautics) Journal, v 14, n 9, September 1976, p 1642-1644.

28. P. Cambray, Measuring thermocouple time constants: a new method, Combustion Science and Technology, v 45, 1986, p 221-224.

29. L. J. Forney, G. C. Fralick, Two wire thermocouple: frequency in constant flow, Review of Scientific Instruments, v 65, n 10, October 1994, p 3252-3257.

30. M. Tagawa, Y. Ohta, Two-thermocouple probe for fluctuating temperature measurement in combustion – Rational Estimation of mean and fluctuating time constants, Combustion and Flame, v 109, n 4, June 1997, p 549-560.

31. P. A. Santoni, T. Marcelli, E. Leoni, Measurement of fluctuating temperatures in a continuous flame spreading across a fuel bed using a double thermocouple probe, Combustion and Flame, v 131, n 1-2, October 2002, p 47-58.

32. J. R. Louis, W. E. Hartman, The determination and compensated of temperature sensor transfer functions, ASME Paper 64-WA/AUT-13, 1964.

33. N. R. Johnson, A. S. Weinstein, F. Osterle, The influence of gradient temperature fields on thermocouple measurements, ASME Paper 57-HT-18, Aug. 1975.

34. I. Lefkowitz, Methods of dynamic analysis, Instrument Society of America - Journal, v 2, n 6, June 1955, p 203-205.

35. C. E. Shepard, I. Warshawsky, Electrical techniques for time lag compensation of thermocouples used in jet engine gas temperature measurements, Instrument Society of America - Journal, v 9, November 1953, p 119-124.

36. I. Warshawsky, On-line dynamic gas pyrometry using two-thermocouple probe, Review of Scientific Instruments, v 66, n 3, March 1995, p 2619-2624.

37. M. Vachon, P. Cambray, T. Maciaszek, J. C. Bellet, Temperature and velocity fluctuation measurements in a diffusion flame with large buoyancy effects, Combustion Science and Technology, v 48, 1986, p 223-240.

38. S. B. S. Chandran, N. M. Komerath, W. M. Grissom, J. I. Jagoda, W. C. Strahle, Time resolved thermometry by simultaneous thermocouple and rayleigh scattering measurments in a turbulent flame, Combustion Science and Technology, v 44, 1985, p 47-60.

39. F. C. Lockwood, H. A. Moneib, Fluctuating temperature measurements in a heated found free jet, Combustion Science and Technology, v 22, 1980, p 63-81.

40. D. Wang, M. Wang, G. T. Reader, M. Zheng, A numerical study on uncontrolled regeneration processes in diesel particulate filters, 2004 ASME-IEC Fall Technical Conference Proceedings, 2004.

41. J. P. Holman, Experimental methods for engineers, McGraw-Hill Companies, Inc., ISBN 0-07-366055-8, 2001.

APPENDICES

APPENDIX A: Front Panels of LabVIEW VIs

1. Front Panel of the Thermocouple Signal Acquisition Program

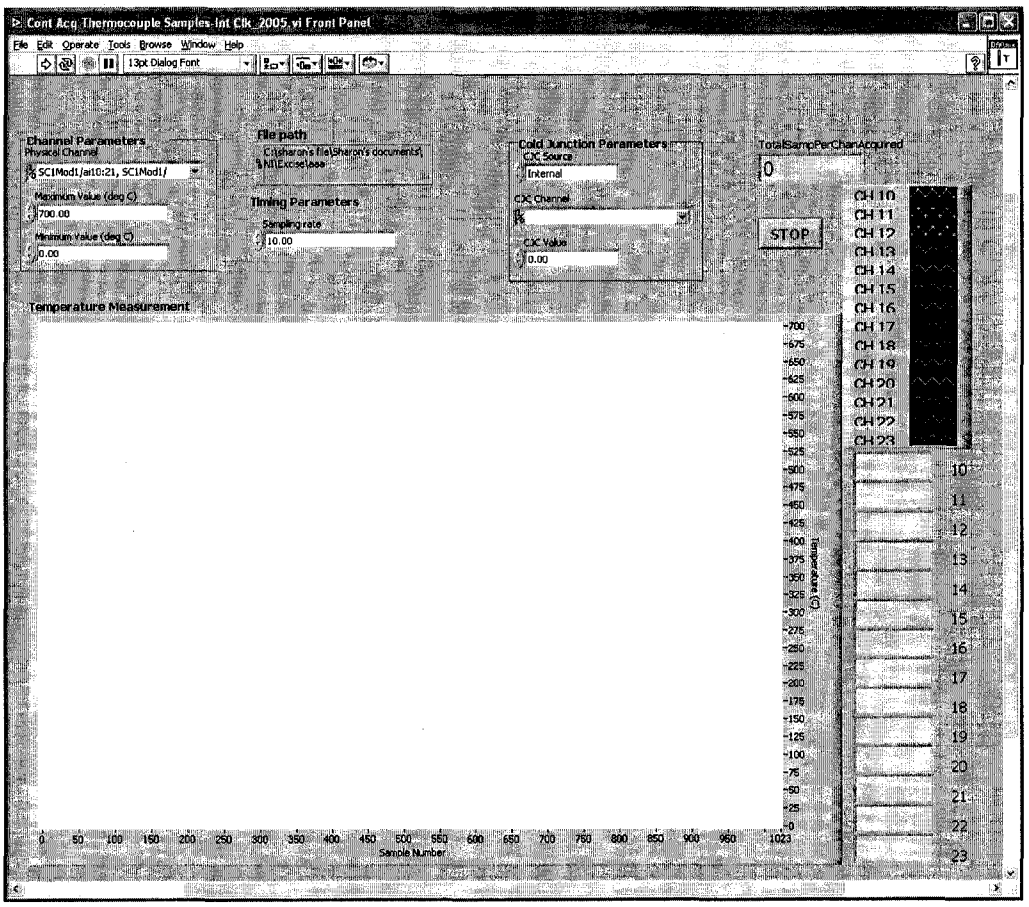

2. Front Panel of the Finite Fuel Injection Digital Pulse Train Program

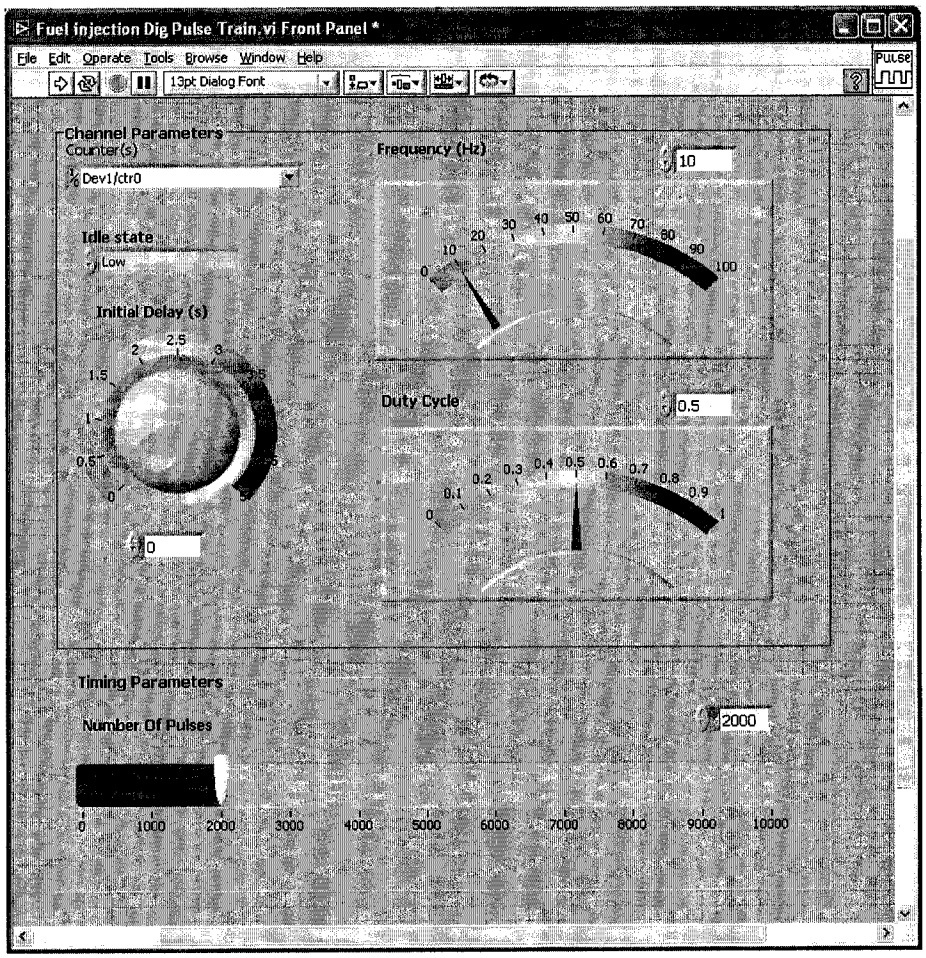

3. Front Panel of the Decision-Making Program of the Simple Closed Loop System

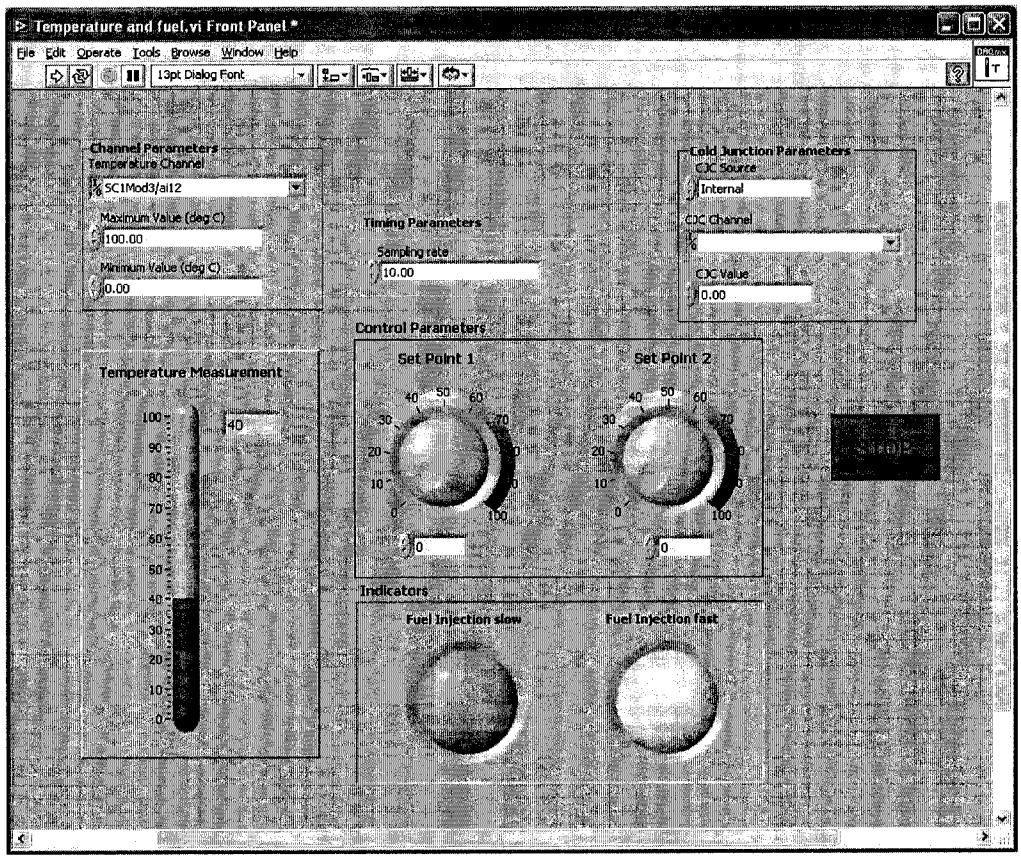

4. Front Panel of the Solenoid Valve Control Program

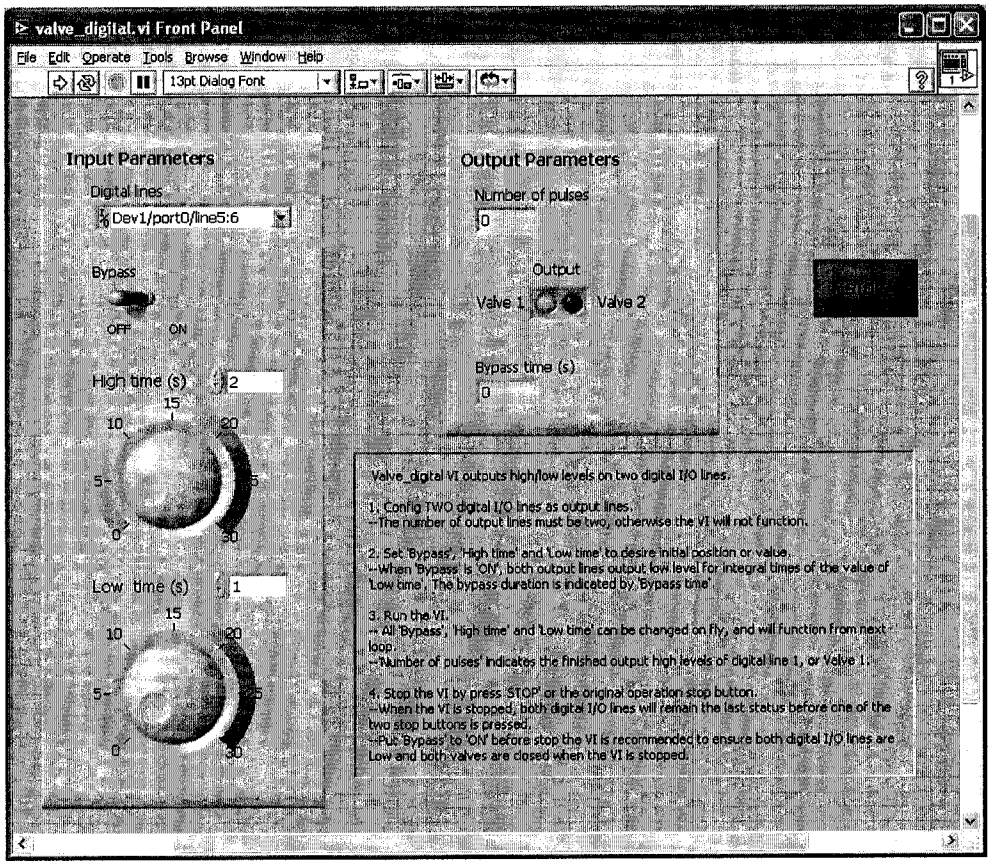

5. Front Panel of the Real-Time Temperature Estimation Program with Two Two-Thermocouple Combinations and One Single Thermocouple Calculation

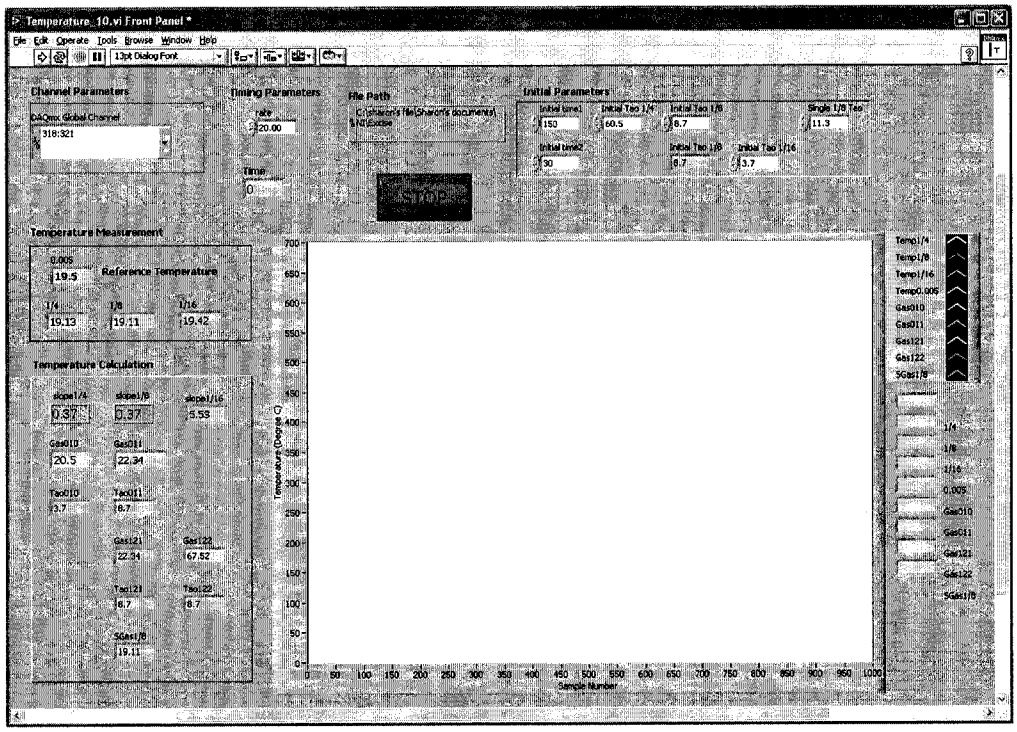

APPENDIX B: Error Analysis

A number of error sources that may cause uncertainty in the measurement of the exhaust gas temperature present in the current experimental setup of the temperature measurement. The thermocouples used in the experiments may cause one of the error sources. Although the thermocouples are all type-K, they give different readings for the same steady temperature because each thermocouple junction is formed differently. According to the manufacturer, the standard error limit of type-K thermocouples is 2.2°C or 0.75% whichever is greater [9]. For the exhaust gas temperature range of the Yanmar diesel engine, from 100°C to 700°C, the error limit is between 2.2°C to 5.25°C depends on the exhaust gas temperature. This type of error may be reduced by the calibration or software compensation.

To connect the thermocouples to the data acquisition system, type-K thermocouple extension wires and connectors are used. Because of the different connections between the thermocouples and the extension wires and the different length of the thermocouple extension wires, random errors may be generated.

The cold-junction compensation of the thermocouple temperature measurement is provided by the data acquisition system. The NI SCXI-1102 thermocouple module reads the cold-junction sensor from the NI SCXI-1303 terminal block along with other thermocouple channels [15]. The error of the cold-junction compensation will be passed to the thermocouple temperature measurement. Although the data acquisition system

employs such procedures as an instrumentation amplifier and a 2 Hz low pass filter for each thermocouple channel to reduce the errors of the measurement, some errors may be produced during the processing of the electrical signals. For instance, because of the limited input resolution of the multifunction data acquisition board NI PCI-6023E, some errors may be generated.

Besides the error generated in the experimental measurement procedures, additional error may be resulted from the theoretical assumptions made during the modeling process of the thermocouples. Compared to the prevailing effect of the heat transfer by convection across the thermocouple bead, the effects of heat transfer by conduction and radiation are negligible under the experimental conditions of this research. The effects of the conduction and radiation are neglected in the temperature response model. Although this neglect is reasonable, it still brings in additional errors to the compensated exhaust gas temperature when the temperature response model is used.

The total error of the temperature measurement is not the simple accumulation of the errors of every error source [41]. There are many methods to estimate the total error in the experimental results. However, no matter which method is used to calculate the total error, the validity of the experimental results will hold unless the total error and the experimental results are of the same magnitude. For this research, the thick thermocouples are not capable of measuring the fast temperature fluctuations in the engine exhaust stream while the compensated exhaust gas temperature calculated with the

temperature response model can indicate the sudden temperature change promptly with good accuracy. For instance, as shown in Figure 4-8, from t = 353.5s to t = 354.5s, when the exhaust gas temperature, which is represented by the reading of the high sensitivity 0.005" diameter thermocouple, suddenly increases from 201.9°C to 357.0°C, the temperature measurement of the 1/8" diameter thermocouple only has changed 9.3°C from 205.1°C to 214.4°C. The error of the temperature measurement with the thick thermocouple is 135.6°C at t = 354.5s. However, the compensated exhaust gas temperature sharply rises from 225.9°C to 353.4°C during the same time period as shown in Figure 4-10. The error between the compensated exhaust gas temperature and the directly measured exhaust gas temperature is only 3.6°C at t = 354.5s. Actually, for all the engine tests in this research, the difference between the compensated exhaust gas temperature and the temperature measurement recorded simultaneously by the high sensitivity thermocouple representing the real-time temperature value is less than 3% of the total exhaust gas temperature range. It is obvious that the implementation of the temperature response model has improved the temperature measurement accuracy dramatically.

VITA AUCTORIS

NAME: Yue Wu

PLACE OF BIRTH: Changsha, Hunan Province, China

YEAR OF BIRTH: 1971

EDUCATION: Beijing Institute of Technology, Beijing, China

1988-1992 B. Sc.

Beijing Institute of Technology, Beijing, China

1992-1995 M. Sc.

University of Windsor, Windsor, Ontario, Canada

2003-2005 M. A. Sc.